
**ISAS - INTERNATIONAL SCHOOL FOR ADVANCED STUDIES**


# Correlated Basis Function Method for Fermions on a Lattice: Applications to the Hubbard Model

Thesis submitted for the degree of

"Doctor Philosophiæ"


CANDIDATE

Xiaoqian Wang

SUPERVISORS

Prof. E. Tosatti

Prof. S. Fantoni



October 1989

TRIESTE



SA - SCUOLA
ERNAZIONALE
SUPERIORE
UDI AVANZATI
TRIESTE
Strada Costiera 11

Scuola Internazionale Superiore di Studi Avanzati

International School for Advanced Studies

# Correlated Basis Function Method for Fermions on a Lattice: Applications to the Hubbard model

Thesis submitted for the degree of

"Doctor Philosophiæ"

CANDIDATE

Xiaoqian Wang

SUPERVISORS

Prof. E. Tosatti

Prof. S. Fantoni

October 1989

# Contents

## Abstract

We introduce a new lattice version of the Correlated Basis Function (CBF) approach for the study of strongly interacting electrons. As a first application we have chosen the 1 dimensional Hubbard model. For this system, we have implemented different types of correlations, namely a) Gutzwiller; b) Jastrow; c) nearest-neighbor spin-spin; and d) excitonic ("e-d") on the Fermi sea. Correlated BCS and Spin-Density-Wave (SDW) theories have also been developed. The resulting energies, momentum distribution and other quantities are compared with exact results (when available), and are discussed, both from the point of view of the method, as well as from a physical view point. The most important correlations that are needed to obtain good ground state energies are found to be Gutzwiller (reduced double occupancy) plus "ed" attractive correlations (between empty and doubly occupied sites), in agreement with other studies.

# Acknowledgments

I would like to exress my cordial thanks to Professors Erio Tosatti and Stefano Fantoni, who introduced me to this field of research, guided me at every stage of this work and read the manuscript critically. I am very grateful to Professor Yu Lu, who kindly advises me and often responds to my elementary questions without reluctance. I appreciate fruitful discussions with Dr. Michele Viviani at the early stage of this work. Although I do not write down their names, I express my gratitude to many researchers who discussed with me and made useful comments on this work.

This work has been in part supported by the SISSA-CINECA (Centro di Calcolo Elettronico dell'Italia Nord-Orientale) collaborative project, under the sponsorship of the Italian Ministry for Public Education.

# Chapter 1

# Introduction

## 1.1 Hubbard model

The effect of strong correlation between electrons is one the most important issues which remains challenging in solid state physics. Many significant phenomena, such as magnetism of itinerant electrons in transition metals and compounds and metal-insulator transitions arise from this effect. Moreover recent developments have revealed that heavy electron systems and high- $T_c$ superconductors may have to be added to this list.

The Hubbard model [1][2], given by

$$H = -t \sum_{<i,j>,\sigma} c^{\dagger}_{i\sigma} c_{j\sigma} + U \sum_{i} n_{i\uparrow} n_{i\downarrow}, \tag{1.1}$$

here $i, j$ are sites of a $D$-dimensional lattice, $t$ is the electron hopping energy, and $U$ is the on-site repulsion, is a well-known prototype problem of highly interacting electrons. The first part of Eq. (1.1) is the kinetic energy due to the hopping between sites $i$ and $j$, which can be expressed in momentum

representation in the form

$$T = \sum_{\mathbf{k},\sigma} \epsilon(\mathbf{k}) c^{\dagger}_{\mathbf{k}\sigma} c_{\mathbf{k}\sigma}, \tag{1.2}$$

with

$$\epsilon(\mathbf{k}) = -tN^{-1} \sum_{i,j} \exp(-i\mathbf{k}(\mathbf{R_i} - \mathbf{R_j})) \tag{1.3}$$

and

$$c_{\mathbf{k}\sigma} = N^{-1/2} \sum_{i} c_{i\sigma} \exp(-i\mathbf{k}\mathbf{R_i}), \tag{1.4}$$

etc. This term makes the model inherently quantum mechanical. The interaction part reads $U \sum_i c^{+}_{i\uparrow} c_{i\uparrow} c^{+}_{i\downarrow} c_{i\downarrow}$ and formally represents a four-fermion operator. Both the $U \to 0$ and $U \to \infty$ limits are simple to visualize. For $U = 0$ the ground state is given by

$$|\Psi_0> = \prod_{k<k_F} c^{\dagger}_{k\uparrow} c^{\dagger}_{k\downarrow} |0>, \tag{1.5}$$

corresponding to a Slater determinant of extended Bloch functions. For $U \to \infty$ only those configurations which do not have doubly occupied sites survive. There is an important difference between the two limits. For $U \to 0$ the ground state is not degenerate. For $U \to \infty$ there is a huge degeneracy both due to the distribution of particles and due to the spin configurations. The former type of degeneracy is absent for the particular case of an average density of one particle per site ("half-filled band"). The remaining problem of spin degeneracy can be mapped onto a Heisenberg model with antiferromagnetic exchange. As simple as this Hamiltonian is, apart from Lieb and Wu's exact result in $D = 1$ dimension [3], the deep physics of this model is still open to discussion. In recent times, interest in

the Hubbard model has been revived by Anderson's suggestion [4] that non-Fermi liquid behavior away from 1/2 filling might be at the origin of high $T_c$ superconductivity. The resulting literature has acquired enormous proportions [7]. Most notable in this literature are recently developed methods (like QMC methods [8]) of numerical solution [6] [8], and also variational approaches [9]. The variational approaches, in particular, have been very useful in substantiating ideas on the importance of BCS-like correlations (as postulated by the RVB state [5] of Anderson).

## 1.2 CBF method to Hubbard model

The well-known CBF method [10][11] can be used to go beyond the variational procedure. Widely used for continuous models of interacting fermions such as nuclear matter [13] and liquid $^3$He [12], it has never been implemented so far for a discrete lattice model. Yet, its potential usefulness for a lattice problem like the Hubbard model seems to exist. Unlike variational Monte Carlo methods [9], where the expectation values of important physical operators are evaluated by stochastic methods, in the CBF method these expectations are calculated using diagrammatic expansions, and the FHNC method [14] [15] which sums up all the important class of diagrams. This expansion can be done at the outset in the thermodynamic limit, and is thus not disturbed by finite size problems, which instead hamper the stochastic approaches. Also, higher dimensionalities are not a big problem in the FHNC/CBF method, while their difficulty becomes rapidly prohibitive in the stochastic methods.

On the other hand, the FHNC diagrammatic expansion at present cannot be expressed in a fully closed form, which makes this approach intrinsically approximate. Higher levels of approximations, although formally doable, require increasing amount of analytical work. By contrast, the accuracy of stochastic methods is in principle limited only by the computer capabilities.

In practice, our CBF variational state is taken to be of the form

$$|\Psi >= G|\Phi >, \tag{1.6}$$

where $|\Phi >$ is some reference state and $G$ denotes correlations to be built into that state, which however cannot be too strong to change the symmetries as well as the character of $|\Phi >$. This fact must in particular be borne in mind when examining all results obtained when $|\Phi >$ is a Fermi sea: the approximate correlations of $|\Psi >$ will invariably conserve a remnant of Fermi-liquid character, unless extremely specific correlations are built in, or the CBF perturbation theory is fully used.

In this thesis, we describe a first systematic attempt at applying the FHNC/CBF method to the discrete 1-Dimensional Hubbard model (1.1). The main scope of this exercise is not to uncover any new physics of this particular situation, which is rather well studied. On the contrary, we wish to use this calculation to assess the applicability and limitations of the method, and to obtain precise indications which will serve for the future planning of calculations aimed at extracting new physics for the Hubbard model in $D > 1$ dimensions. More specifically, we shall describe here calculations where $|\Phi >$ of Eq.(1.6) is taken to be the unperturbed 1-D Fermi

sea, and G will correspond to various correlations of increasing richness, beginning from Gutzwiller [9][16], to Jastrow [10], to include the so-called $e-d$ correlations [20], to spin-spin correlations [17]. Because of this choice, all results will bear the Fermi-liquid character by construction, which, strictly speaking, is incorrect at least in $1D$ [21][4]. However, that does not mean that FHNC/CBF is hopelessly wrong. At the price of some increase in complication, as outlined in Chapter 6 and 8, we can perform other calculations with a different choice of $|\Phi>$, for example $|\Phi>=|BCS>$, or $|SDW>$, where the Fermi-liquid character is not present at all (here $|BCS>$ stands for the standard superconducting state [9] and SDW for the standard band antiferromagnetic state [9]). The sense of restricting these first calculations mostly to $|\Phi>=|Fermi\ sea>$ is therefore that of demonstrating the method in its simplest implementation.

## 1.3 Outline of the thesis

The rest of this thesis is organized as follows. The CBF method is formulated and developed for the Hubbard model in Chapter 2. Some of the technicalities which occur in that Chapter are omitted for better readability, and confined to Appendices. In Chapter 3, we describe calculations performed with Gutzwiller and more generally with Jastrow correlations. The convergence of the diagrammatic expansion is first of all tested by comparing FHNC/0 with FHNC/4 [22]. Then physically interacting quantities, like total, kinetic and potential energies, momentum distribution, pair correlations, and effective excitation spectrum are presented in detail.

The improvement in going from Gutzwiller to Jastrow is investigated, and found to be rather small [23]. In Chapter 4, the so-called $e-d$ correlations between an empty site ($e$) and a doubly occupied site ($d$) earlier recognized to be very important near 1/2 filling [25] are implemented, by introducing four-site (quartet) correlation terms in G. The resulting energetic improvement is, as expected, quite satisfactory. Also changes of momentum distribution are evaluated and discussed. In Chapter 5, we briefly consider the problem of spin-spin correlations. Since in the present problem their impact is not very large, we limit ourselves to a rather simple analytic treatment. Future investigations of e.g. the magnetic phase diagram for $D > 1$ would of course require a better treatment than that. Chapter 6 contains an outline of the FHNC/CBF methods applied to an alternative reference state $|\Phi >= |BCS >$, which may be suitable for , e.g., RVB studies in $D = 2$ and which we are considering as a future application. Some preliminary results for small $U/t$ values are also presented. In Chapter 7, we develop the correlated spin-density-wave (SDW) theory, and its application to the $1D$ Hubbard model is presented and discussed. Finally, discussions and the conclusions of this work are presented in Chapter 8.

# Chapter 2

# The CBF method for lattice calculation

## 2.1 The CBF theory

The Correlated Basis Function theory [24] makes use of correlated wave function of the type

$$\bar{\Psi}_n = G\Phi_n / < \Phi_n^* G^\dagger | G\Phi_n >^{1/2} \tag{2.1}$$

to derive the appropriate basis functions of the theory for fermions; $\Phi_n$ are independent particle model fermion wave functions, say Hartree-Fock, Spin Density Wave (SDW), BCS (which is not strictly independent electron but still manageable) etc, and G is an operator which builds up into $\Phi_n$ the important correlations amongst the particles.

The operator $G$ usually contains parameters, whose values are determined variationally, by minimizing the expectation value of the hamiltonian

on the ground state $\bar{\Psi}_0$,

$$E =< \Psi|H|\Psi > / < \Psi|\Psi >, \tag{2.2}$$

with respect to the variational parameters of $G$.

The correlated functions $\bar{\Psi}_n$ are usually not orthogonal each other. They can be orthogonalized in a number of way. However, since the real eigenvalue $E_n$ is in general quite close to $< \bar{\Psi}_n|H|\bar{\Psi}_n >$, one requires that the orthogonal set $|\Psi_n >$ maintains the diagonal matrix elements variational estimated, namely

$$< \Psi_n|H|\Psi_n >=< \bar{\Psi}_n|H|\bar{\Psi}_n > +O(1/A), \tag{2.3}$$

where $A$ is the number of particles. This property is achieved by using the orthogonalization procedure given in Ref. [10]. Standard perturbation techniques are then used to solve the many-body problem, by keeping the diagonal part of $H$ as the unperturbed hamiltonian $H_0$, namely

$$H_{0,ij} = \delta_{ij} < \Psi_i|H|\Psi_j >, \tag{2.4}$$

whilst the interaction term $H_I$ is given by

$$H_{I,ij} = (1 - \delta_{ij}) < \Psi_i|H|\Psi_j > . \tag{2.5}$$

In this thesis we limit our attention to the calculation of the diagonal matrix elements of $H$, in the case of an independent particle model $|\Phi >$ of the Hartree-Fock or of the BCS type. In particular we are interested in a variational calculation of ground state energy $H_{00}$, which will also provide us a realistic correlation operator $G$.

The correlation operator can be written in the following general form:

$$\begin{aligned} G &= G^J \times G^3 \times G^4 \times ... G^{SD} \\ &= \prod_{i,j} f(r_{i,j}) \prod_{i,j,k} f^3(r_{i,j}, r_{i,k}) \prod_{i,j,k,l} f^4(r_{i,j}, r_{j,k}, r_{k,l}) \\ S & \prod_{i,j} (1 + \hat{\eta}_2(i,j)) \end{aligned} \tag{2.6}$$

where $G^J$ (Jastrow), $G^3$ (3-body) and $G^4$ (4-body) are state-independent correlations, determined strictly by interparticle coordinates, while $G^{SD}$ are in general state-dependent correlations, exemplified, in particular, by spin-dependent correlations

$$\hat{\eta}(i,j) = 1 + \eta(r_{ij}) \vec{\sigma_i} \vec{\sigma_j}, \tag{2.7}$$

and $S$ is a symmetry operator. In this Chapter we consider the case of correlation operator of the Jastrow type and a $|\Phi>$ of the Hartree-Fock type. The inclusion of $G^4$ is discussed in Chapter 4 and that of state dependent correlation in Chapter 5. The cases of a $|\Phi>$ of the BCS or SDW type are reported in Chapter 6 and Chapter 7 respectively.

The expectation value of the hamiltonian $H$ is given by

$$E = < T > + < V >, \tag{2.8}$$

$$< T > /N = -2t\rho n(a), \tag{2.9}$$

$$< V > /N = U\rho^2 g(0)/2, \tag{2.10}$$

where $N$ are the lattice points separated by $a$ and $\rho = A/N$, which is twice the filling factor. The functions $g(r_{ij})$ and $n(r_{ij})$ are the pair distribution function and the one body density matrix respectively. As seen from (2.9),

we need to know the former for $r_{ij} = 0$ (on-site resulsion) and the latter for $r_{ij} = a$ (first-neighbor hopping). These two quantities also allows for the evaluation of the density-density correlation function $S(k)$ and the momentum distribution $n(k)$, as will be shown in Chap. 2.3.

## 2.2 Pair correlation function

The derivation of the FHNC integral equations is based on a diagrammatic cluster expansion of the multidimensional integrals which appear in the definition of the two-body radial distribution function (pair-correlation function)

$$g(r_{12}) = \frac{A(A-1)}{\rho^2} \frac{\int dx_3 ... dx_A |\Phi|^2 \prod_{i,j} f^2(r_{i,j})}{\int dx_1 ... dx_A |\Phi|^2 \prod_{i,j} f^2(r_{i,j})}, \tag{2.11}$$

where $A$ is the number of particles and $\rho$ denotes the particle density of the system. the relevant spin summations are implicit in the integrations. In addition to the original papers several review articles are now available in which the FHNC method is explained [22] [24]. Therefore in this section we shall only very briefly illustrate the FHNC method and we refer to the original papers and those review articles for more detailed discussion. In Eq. (2.11), $\Phi$ is taken to be the antisymmetrized product of the following single particle wave functions

$$\psi_{k,\sigma}(i) = e^{ikx_i} \xi_\sigma(i), \tag{2.12}$$

where $\xi_\sigma(i)$ represents the spin state, the the variable $x_i$ sums over the $N$ lattice points and $k$ (1D) is subjected to boundary conditions

$$k_l = l \frac{2\pi}{Na}, \tag{2.13}$$

with $l = \pm 1,\ \pm 2,\ ....$

The fermi momentum $k_F$ is given by

$$k_F = \frac{\rho\pi}{2a}, \tag{2.14}$$

where $\rho$, the density of the system is twice of the filling factor $\nu$.

The correlation function $f(r_{ij})$ is also defined on the lattice points, namely the interparticle distance $r_{ij} = x_i - x_j$ with $x_i = ia$ $(i = 0, \pm 1, ... \pm N)$. Because the convolution integral becomes a product in momentum space, the convolution integral equations can be expressed in momentum space, and thus their extension to the lattice case is straightforward.

In the case of Fermi statistics the pair-correlation function is obtained as a sum of linked irreducible diagrams. In these diagrams a pair of particles may be correlated either by a dynamical correlation $h(r_{ij}) = f^2(r_{ij}) - 1$ or by an oriented statistical correlation or both. The statistical or exchange lines, which appear in nonoverlapping closed loops, correspond to the uncorrelated two body density matrix, is given by

$$\begin{aligned} \rho(x_{ij}) &= \frac{1}{N}\sum_{k,\sigma} \psi^*_{k,\sigma}(i)\psi_{k,\sigma}(j) \\ &= \rho\sum_{\sigma} \xi^*_{\sigma}(i)\xi_{\sigma}(j)\frac{sin(\rho k_F x_{ij})}{k_F x_{ij}} \\ &= \frac{1}{2}\rho(x_{ij})\sum_{\sigma} \xi^*_{\sigma}(i)\xi_{\sigma}(j), \end{aligned} \tag{2.15}$$

with the one body density matrix

$$\rho(i) = \frac{1}{N}\sum_{k,\sigma} |\psi_{k,\sigma}(i)|^2 = \rho. \tag{2.16}$$

Correspondingly, the uncorrelated pair distribution function results to be

$$g(x_{ij}) = 1 - \frac{1}{2}\rho^2(x_{ij}). \tag{2.17}$$

By using Eqs.(2.15, 16) one easily recovers the Hartree-Fock results for the uncorrelated energy $E_{HF} = -4t/\pi + U/4$ at half filling.

In the case $f(r_{ij}) \neq 0$, the pair distribution function can be calculated by using the FHNC theory originally developed to study strong interacting Fermi systems [26][27] by keeping $\rho(x_{ij})$ of Eq. (2.15) as the exchange correlation. In such a theory $g(r)$ is given by a sum of the distribution functions,

$$g(r) = g_{dd}(r) + 2g_{de}(r) + g_{ee}(r), \tag{2.18}$$

where the labels $dd, de$ and $ee$ refer to the particular exchange character of the distribution functions considered. The "direct-direct" diagrams included in $g_{dd}$ have only correlations $h(r_{ij}) = f^2(r_{ij}) - 1$ ending at both external points, whereas the label $e$ indicates that the corresponding diagrams have one exchange correlation $\rho^2(r_{ij})$ ending at the external points. In Appendix $A$ the detail diagrammatic rules for the cluster expansion are discussed.

The various distribution functions are calculated by solving the following set of integral equations (see also Appendix $A$):

$$\begin{aligned} N_{\alpha\beta}(x_{ij}) &= \rho \sum_{\gamma,\gamma'} \sum_{k} (g_{\alpha\gamma}(x_{ik}) - \delta_{\alpha d,\gamma d}) A_{\gamma\gamma'}(g_{\gamma'\beta}(x_{kj}) \\ &- N_{\gamma'\beta}(x_{kj}) + \frac{1}{2}\delta_{\beta c}\delta_{\gamma' c}\rho(x_{kj})) \\ (\alpha\beta) &= dd, de, ee, cc \end{aligned} \tag{2.19}$$

where $k$ run over the lattice points whereas the indices $\alpha, \beta, \gamma, \gamma'$ run over

the exchange labels $(d, e, c)$ and the $3 \times 3$ matrix $A$ is given by

$$A \equiv \begin{pmatrix} 1 & 1 & 0 \\ 1 & 0 & 0 \\ 0 & 0 & 1 \end{pmatrix}. \tag{2.20}$$

The $cc$-function entering in Eq. (2.18) sum up diagrams with one exchange loop joining the two indicated external points. The distribution functions $g_{ab}(x_{ij})$ are given by

$$\begin{aligned} g_{dd}(x) &= f^2(x) \exp\{N_{dd}(x) + E_{dd}(x)\} \\ &= X_{dd}(x) + N_{dd}(x) + 1, \end{aligned} \tag{2.21}$$

$$g_{de}(x) = g_{dd}\{N_{de}(x) + E_{de}(x)\} = X_{de}(x) + N_{de}(x), \tag{2.22}$$

$$\begin{aligned} g_{ee}(x) &= g_{dd}\{N_{ee}(x) + E_{ee}(x) + [N_{de}(x) + E_{de}(x)]^2 \\ &- 2[N_{cc}(x) + E_{cc}(x) - \frac{1}{2}\rho(x)]^2\} \\ &= X_{ee}(x) + N_{ee}(x), \end{aligned} \tag{2.23}$$

$$\begin{aligned} g_{cc}(x) &= g_{dd}\{N_{cc}(x) + E_{cc}(x) - \frac{1}{2}\rho(x)\} \\ &= X_{cc}(x) + N_{cc}(x) - \frac{1}{2}\rho(x). \end{aligned} \tag{2.24}$$

The functions $E_{ab}(x_{ij})$ correspond to the so called "bridge (or "elementary") diagrams", two examples of which are shown in Fig. 2.1. They are expressed in terms of $g_{ab}$, and their full calculation can be expressed in the form

$$E_{ab}(x) = \sum_n E^n_{ab}(x), \tag{2.25}$$

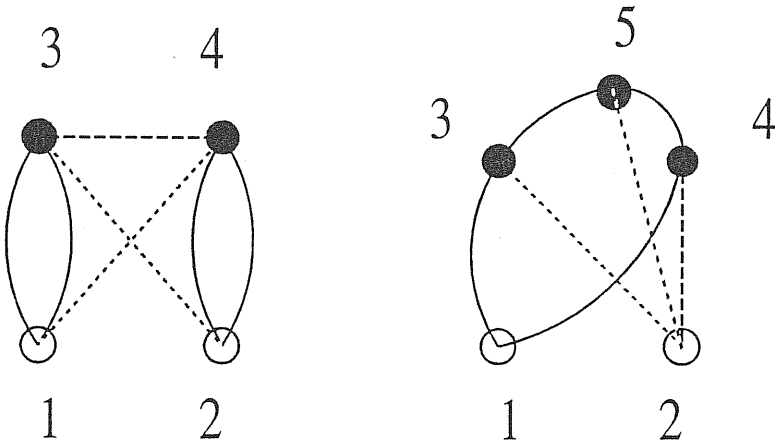


Figure 2.1: Examples of four-body ($a$) and five body ($b$) elementary diagrams, in which each bond can be a different kind of $g$, combined according to the diagrammatic rule, which we discuss in Appendix $A$. Dashed lines are used to represent dynamical correlations $\eta(1,2) = f^2(1,2) - 1$, solid lines correspond to factors $-\rho(k_F x)/2$.

where the index $n$ refer to the number of points which characterizes the corresponding bridge diagrams. For instance diagram $a$ in Fig. 2.1 correspond to $n = 4$, whereas the five body bridge diagram has $n = 5$ (diagram $b$ in Fig. 2.1). If $E_{ab}$ is taken to be zero, the corresponding approximation is called FHNC/0. Similarly the approximation FHNC/N is obtained by truncating the series (2.25) at $n = N$. It is known that the convergence of the series FHNC/n rapidly decreases as the contribution of the bridge diagrams to $g(r)$ increases. Eventually one needs to use different schemes, like for instance the scaling approximation [33] or the interpolation equation method [28]. In this thesis we consider the FHNC/0 and FHNC/4 truncation. The calculation of the four-body bridge diagrams $E^4_{ab}$ is given in Appendix $B$. The lowest order approximation FHNC/0 has been found [12][34] to be accurate for many dense systems like e-plasma, liquid Helium, nuclear matter and neutron matter.

Further, the density-density correlation function $S(k)$ is obtained from the pair correlation function by means of the equation

$$S(k) = 1 + \rho \sum_l (g(x_l) - 1) \exp(ikx_l). \tag{2.26}$$

## 2.3 One body Density matrix

In order to study the kinetic energy of the Hubbard hamiltonian (1.1), it is necessary to evaluate the momentum distribution function. This quantity is related by a Fourier transform to the one body density matrix defined as

$$n(r_{11'}) = \frac{A(A-1)}{\rho^2}$$

$$\times \frac{\int dx_2 ... dx_A \Phi^*(1'2...A) \prod f(r_{1'i}) \prod f(r_{1j}) \prod_{i<j\neq 1,1'} f^2(r_{ij}) \Phi(12...A)}{\int dx_1 ... dx_A \Phi^* \prod f^2(r_{ij}) \Phi} \tag{2.27}$$

The Hartree-Fock approximation is obviously included in $n(r_{11'})$ and it corresponds to the uncorrelated lowest order term of the cluster expansion and it is given in Eq. (2.15).

In analogy to the treatment of the pair-correlation function discussed in the last Section, a diagrammatic expansion of the right-hand side of Eq. (2.27) may be employed to derive a set of integral equations which facilitate the infinite partial summations of the contributing diagrams. The cluster expansion and the FHNC equations to calculate $n(r_{11'})$, have been derived in ref. [27] and they can be readily modified to the present lattice version.

In addition to the dynamical correlation factor $h(r_{ij}) = f^2(r_{ij}) - 1$ the chain and bridge diagrams which contribute to the density matrix contain another dynamic link representing the factor $\xi(r_{ij}) = f(r_{ij}) - 1$. This link originates from the point 1 or 1' and may also be multiplied by statistical correlations: $\xi(r_{ij})\rho(r_{ik})$. Examples of the diagrams as well as detailed discussions of the diagrammatic rules can be found in Refs. [13] and [27]. The diagrams are labelled with $\xi d, \xi e, \xi\xi, \xi cc$, and $\xi c\xi c$ respectively. The density matrix is given by

$$n(r_{11'}) = n_0\{\rho(r_{11'})/2 - N_{\xi c\xi c}(r_{11'}) - E_{\xi c\xi c}(r_{11'}\}exp\{N_{\xi\xi}(r_{11'}) + E_{\xi\xi}(r_{11'})\}, \tag{2.28}$$

where the $\xi c\xi c$ nodal function $N_{\xi c\xi c}$ is obtained by solving the equation:

$$\begin{aligned} N_{\xi c\xi c}(r_{11'}) &= \rho\sum_k\{g_{\xi cc}(r_{1k})(g_{\xi cc}(r_{k1'}) - N_{\xi cc}(r_{k1'}) + \frac{1}{2}\rho_{\xi cc}(r_{k1'})) \\ &- \frac{1}{2}(g_{\xi cc}(r_{1k}) - g_{cc}(r_{1k}) - N_{\xi cc}(r_{1k}) \\ &+ N_{cc}(r_{1k}))\rho(r_{k1'})\}, \end{aligned} \tag{2.29}$$

and the other chain functions for the nodal functions $N_{\xi\xi}, N_{\xi d}, N_{\xi e}$ and $N_{\xi cc}$ are given by Eq. (2.19), where $m$ still runs over $d, e$ or $c$ and $(ab) = \xi\xi, \xi d, \xi e$ and $\xi cc$. The various distribution functions are given by

$$g_{\xi d}(x) = f(x)\exp\{N_{\xi d}(x) + E_{\xi d}(x)\}, \tag{2.30}$$

$$g_{\xi e}(r) = g_{\xi d}(x)\{N_{\xi e}(x) + E_{\xi e}(x)\}, \tag{2.31}$$

$$g_{\xi cc}(r) = g_{\xi d}(x)\{N_{\xi cc}(x) + E_{\xi cc}(x) - (1/2)\rho(x)\}. \tag{2.32}$$

The strength factor of the density matrix $n_0$ may be evaluated as

$$n_0 = e^{2U_\xi - U_d}, \tag{2.33}$$

where

$$\begin{aligned} U_\xi &= \sum_k\{\sum_m(g_{\xi m}(x_{ik}) - N_{\xi d}(x_{ik}) - E_{\xi d}(x_{ik})) \\ &- \sum_{mm'} g_{\xi m}(x_{ik})A_{mm'}(\frac{1}{2}N_{m'\xi}(x_{ki}) + E_{m'\xi}(x_{ki})\} + E_\xi, \end{aligned} \tag{2.34}$$

where both $m$ and $m'$ run over $d$ and $e$ only, and the expression of $U_d$ is obtained from Eq. (2.34) by replacing each subscript $\xi$ with $d$ which means that $U_d$ is determined solely in terms of the diagrams which contribute to the pair correlation function. The expressions of the bridge functions appearing in the calculation of $n(r)$ are given in Appendix B.

The momentum distribution is easily calculated from $n(r_{11'})$ by using the following equation

$$n(k) = \frac{1}{2}\sum_i n(x_i) exp(ikx_i). \tag{2.35}$$

The momentum distribution of a normal Fermi system shows a discontinuity at the Fermi surface, which can be calculated through (2.28) and (2.29). The existence of such a discontinuity is the characteristic behavior of a Fermi liquid, and the amount of the discontinuity decreases with increasing strength of the dynamic correlations of the system. However, it is worthnoting that such a discontinuity does not exist if we choose the $\Phi$ of either a BCS or a SDW form, which we will discuss in Chapter 6 and Chapter 7 in more detail.

# Chapter 3

# Gutzwiller and Jastrow correlations

## 3.1 Gutzwiller correlations

Among several approximate methods the variation theory is featured by a wide applicability ranging from weak to strong correlation. A standard approach along this line is to use the Jastrow-type variational wave function [10]

$$\Psi = \prod_{i \leq j} f(r_{ij}) det M, \tag{3.1}$$

where $f(r_{ij})$ is a two-particle correlation factor and det $M$ is the Slater determinant of plane-wave states. The factor $f(r_{ij})$ takes care of strong repulsion acting for a close pair. The Gutzwiller theory is the simplest version of Eq. (3.1) in that only the same site is taken into account in $f(r_{ij})$ (i.e. $f(r_{ij}) = 1$ for $r_{ij} \neq 0$). The resulting wave function is very attrac-

tive in its simplicity. However, even with this simplification, an analytic evaluation of expectation value of energy and other physical quantities is extremely difficult. This led Gutzwiller to resort to a random-phase-type approximation (often called "Gutzwiller approximation"), which turns out to spoil in some cases the upper bound property, a necessary condition for a correct variational theory. Since then many researchers have followed the Gutzwiller approximation (GA), but there are fewer studies which go beyond the approximation. Recently, Vollhardt and his collaborators [16] have worked out analytically the energy and correlation functions for 1D Hubbard model under the Gutzwiller wave function and avoiding the GA. We propose therefore to compare our results with theirs, as a check of the method.

The Gutzwiller ansatz for a state independent correlation operator is of the form [9]

$$G_G = \prod_{ij} f_G(\mathbf{r}_{ij}) = \prod_{ij}(1-(1-g)\delta_{r_{i\uparrow}r_{j\downarrow}}), \tag{3.2}$$

i.e., it correlates only particles sitting on the same site. The limiting values $g = 1$ and $g = 0$ correspond respectively to the uncorrelated Hartree-Fock wave function and to projecting out configurations with double occupancies.

We have performed FHNC/0 and FHNC/4 calculations as a function of $U/t$ and of the filling factor, in order to study the convergence of the FHNC scheme with respect to the inclusion of bridge diagrams. The results of the density-density correlation function $S(k)$ are displayed in Figs.3.1 and 3.2 for $\rho = 1$ and $\rho = 1/2$ respectively. The contribution of bridge diagrams increases for larger value of filling factor and smaller values of $g$.

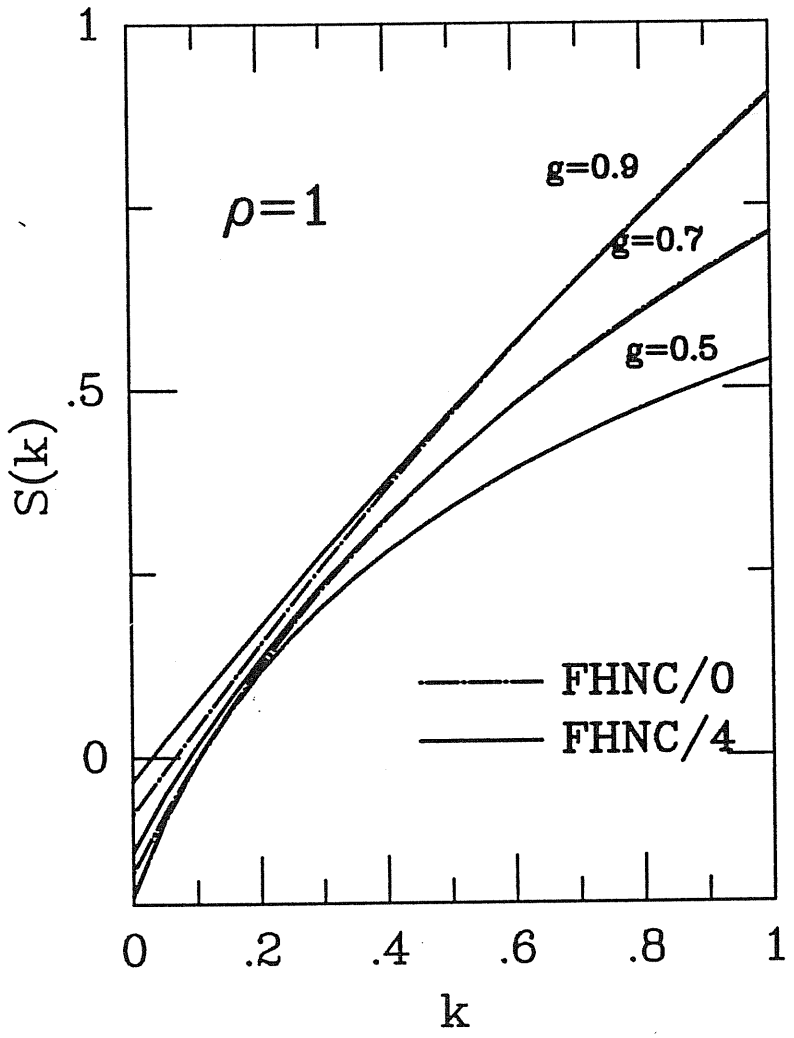


Figure 3.1: Density-density correlation functions for $\rho = 1$. Solid lines correspond to calculations with use of FHNC/4 whereas dashed lines FHNC/0. Results for the Gutzwiller variational parameter $g = 0.9, 0.7$ and $0.5$ are shown.

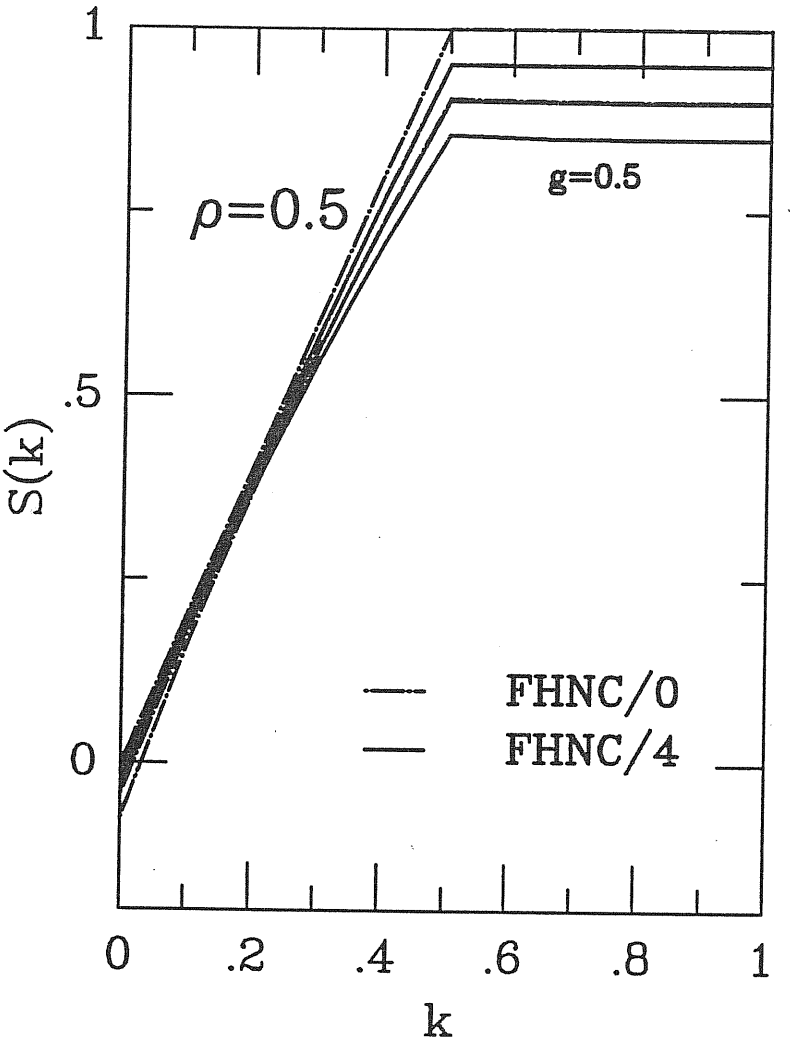


Figure 3.2: Density-density correlation functions for $\rho = 0.5$. Solid lines correspond to calculations with use of FHNC/4 whereas dashed lines FHNC/0. Results for Gutzwiller variational parameter $g = 0.9, 0.7$ and $0.5$ are shown. Note the supression of the $2k_F$ singularity with increasing correlations.

Table I:

Kinetic and potential energies compared with exact results [4] for Gutzwiller wave function.

| | $T_{exact}$ | $V_{exact}$ | T | V | $\rho$ | $n(0)$ |
|---|---|---|---|---|---|---|
| | -.541 | .283 | $-.552$ | .293 | 1.0 | .99 |
| $U/t = 4$ | -.654 | .141 | $-.662$ | .148 | 0.8 | .79 |
| | -.769 | .0658 | $-.770$ | .0659 | 0.6 | .60 |

Their effect is negligible for $|k| > \frac{1}{2}\rho k_f$. The inclusion of four body bridge diagrams helps in reducing the violations of the sum rule $S(0) = 0$. For values of $g < 0.5$ higher order bridge diagrams would be needed in order to fulfill the sum rule. In fact we could force $S(0)$ to be zero by redefining $S(k)$ in a small region of $k$ around 0, with practically no change of the energy expectation values. We have checked that this procedure does not lead to significant energy improvements, and we decided not to follow it.

Violations of similar order of magnitude are found for other sum rules, like for instance, $n(0) = \rho$. As mentioned in the Introduction, such violations are intrinsic in the truncation of the FHNC method, and, if not too large, they do not imply any serious prejudice on the quality of the calculation. Table I reports the results expectation values of the kinetic and potential energies $< T > /N$ and $< V > /N$ compared with exact results. The inclusion of bridge diagrams improves slightly the accuracy of the calculation. Somewhat surprisingly, the improvement is substantial for "weak"

correlations, i.e., $g > 0.5$. In the case of strong correlation this result indicates the convergence of the FHNC scheme is getting lower and lower and eventually one should eventually resort to other schemes [10][19][28]. As a measure of the importance of bridge diagrams, we note that the relative importance of bridge diagrams, given by the ratio $E_{dd}/N_{dd}$ increases for smaller values of $g$ (stronger correlations), as expected. Similar results are found for other elementary functions $E_{de}, E_{ee}$ and $E_{cc}$.

For a given value of $U/t$ and of $\rho$ we have minimized total energy, i.e., the FHNC/4 estimated expectation value of the Hubbard hamiltonian (1.1), with respect to the variational parameter $g$. The results obtained are given in Fig. 3.3 and compared with the "exact Gutzwiller" results [16] and also with values obtained from Lieb and Wu's exact formulas. For $U/t$ up to about 5, our results are almost identical to the Gutzwiller results [16], obtained with the same wave function. For larger $U/t$, higher order bridge diagrams are clearly needed. It has to be noticed that the accuracy for the total energy is substantially better than the corresponding accuracy found separately for $< T >$ and $< V >$ as shown in Table I. The kinetic energy is too low, since correlations are imperfectly implemented. The potential energy is correspondingly too high, and largely compensates the kinetic energy error, but of course not exactly so.

The FHNC/4 estimates of $n(k)$ for $g = 0.3$ and $0.6$ at $\rho = 0.8$ are compared with the corresponding "exact Gutzwiller" results in Fig. 3.4. The increasing behavior of $n(k)$ with $k$ is a typical defect of the Gutzwiller ansatz [25] and is present in our calculation too, especially before the $k_F$ jump. As we will show in the next Chapter the inclusion of quartet corre-

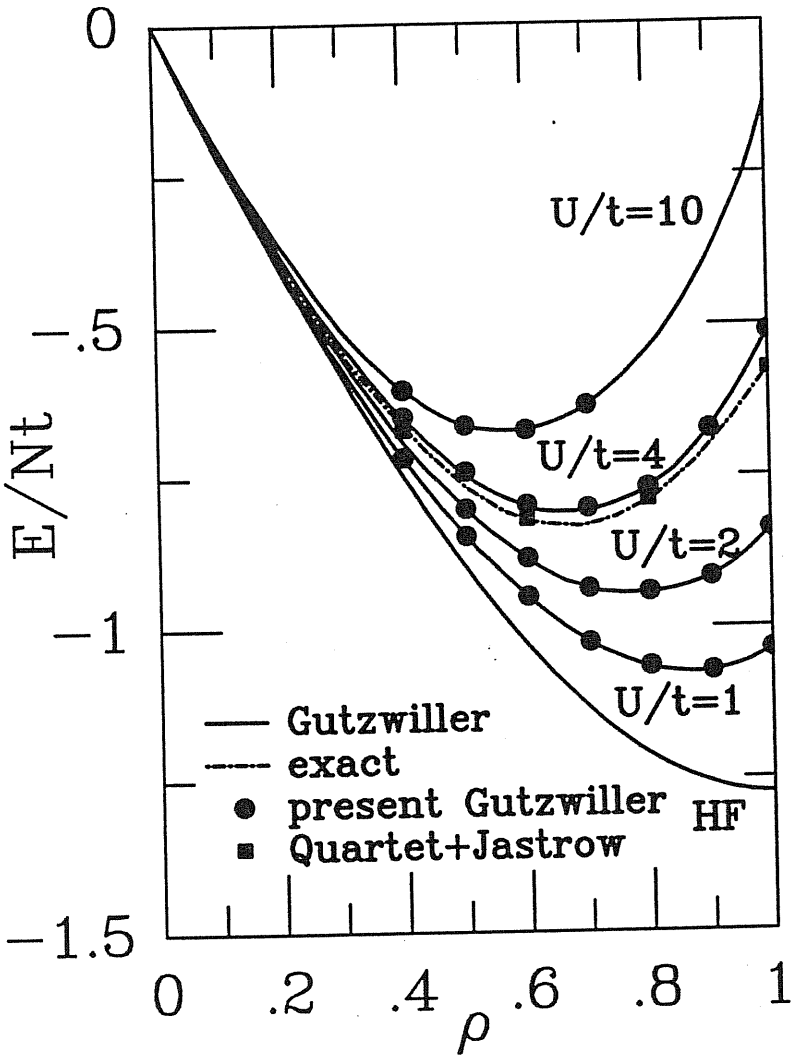


Figure 3.3: Total energy for the Gutzwiller wave function compared with the exact Gutzwiller results.

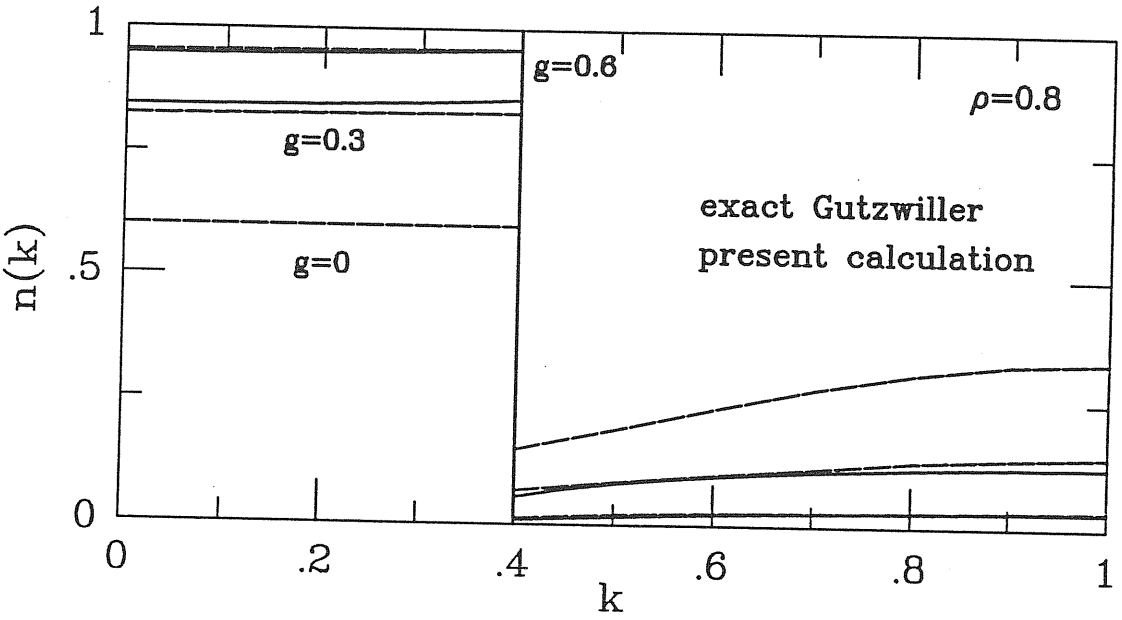


Figure 3.4: Momentum distribution function evaluated by the present method (dashed lines) for $\rho = 0.8$ compared with the exact results for the same Gutzwiller wave function [16] (solid lines).

lations acts to remove this behavior.

## 3.2 Single particle excitation spectrum

We have calculated the single particle excitation spectrum $e(k)$, by evaluating the diagonal matrix elements of the hamiltonian on correlated particle-hole states of the type given in Eq. (2.1). The correlation operator $G$ used is of the Gutzwiller type with the parameter $g$ determined by variational calculation in the ground state previously discussed. The particle-hole uncorrelated wave function $|\Phi_n>$ corresponds to a state with the particle having momentum $p$ and the hole momentum $k = k_F$

$$\epsilon(p > k_F) - \epsilon(p = k_F) = \frac{< \Phi_{ph} G^\dagger | H | G \Phi_{ph} >}{< \Phi_{ph} | \Phi_{ph} >^{1/2}}. \tag{3.3}$$

The actual calculation has been performed [28] by keeping the following density matrix

$$\rho_{p,\Delta}(x_{ij}) = \rho(x_{ij}) - \Delta(\cos p x_{ij} - \cos k_F x_{ij}) \tag{3.4}$$

in place of $\rho(x_{ij})$ of Eq. (2.15). That amounts to remove a state for $k = k_F$ and putting it into $p$. Having created this "bare" elctron-hole pair into the uncorrelated function $\Phi_{ph}$, then the rest of the correlation calculation is repeated exactly as for the ground state. One has

$$\epsilon(p) - \epsilon(k_F) = \frac{\partial}{\partial \Delta}(E(\rho_{p,\Delta}) - E(\rho))\,|_{\Delta=0} \tag{3.5}$$

A completely similar procedure has been used to calculate the energy of the hole states $k < k_F$.

The single particle excitation spectrum $e(k)$ is displayed in Fig. 3.5 and 3.6 for different values of $U/t$ and for $\rho = 1$ and $1/2$ respectively. It is interesting to note that the slope of $U/t$ for $k \sim k_F$ increases with $U/t$, in qualitative agreement with the behavior expected from perturbative (e.g. one loop) self-energy diagram. This increase of slope goes qualitatively in the right direction, and indicates a tendency to develop a pseudogap. That pseudogap in turn is a remnant of the true gap $\Delta$ that could be obtained by implementing the exact (Lieb-Wu) correlations at $\rho = 1$. Such a striking disagreement between the known exact result (a true gap in $e(k)$) and our calculation exhibiting only slight steepening over the free particle $e(k)$ should not be surprising. This defect is intrinsic and well-known for the Gutzwiller wave function.

Away from half filling ($\rho < 1$), the change of $e(k)$ with increasing correlations is again similar, but is asymmetric for electrons and holes. As it turns out, and is shown in Fig. 3.6, correlation effects are far larger for holes than for electrons. Again, the Gutzwiller approximation fails to yield the more delicate aspects of the 1D Hubbard model, which implies the total absence of quasi-particles [30], which makes $e(k)$ itself ill-defined.

## 3.3 Jastrow correlation

The results presented so far applied to the strictly on-site Gutzwiller correlation (3.1). Next we have studied the possible importance of nearest-

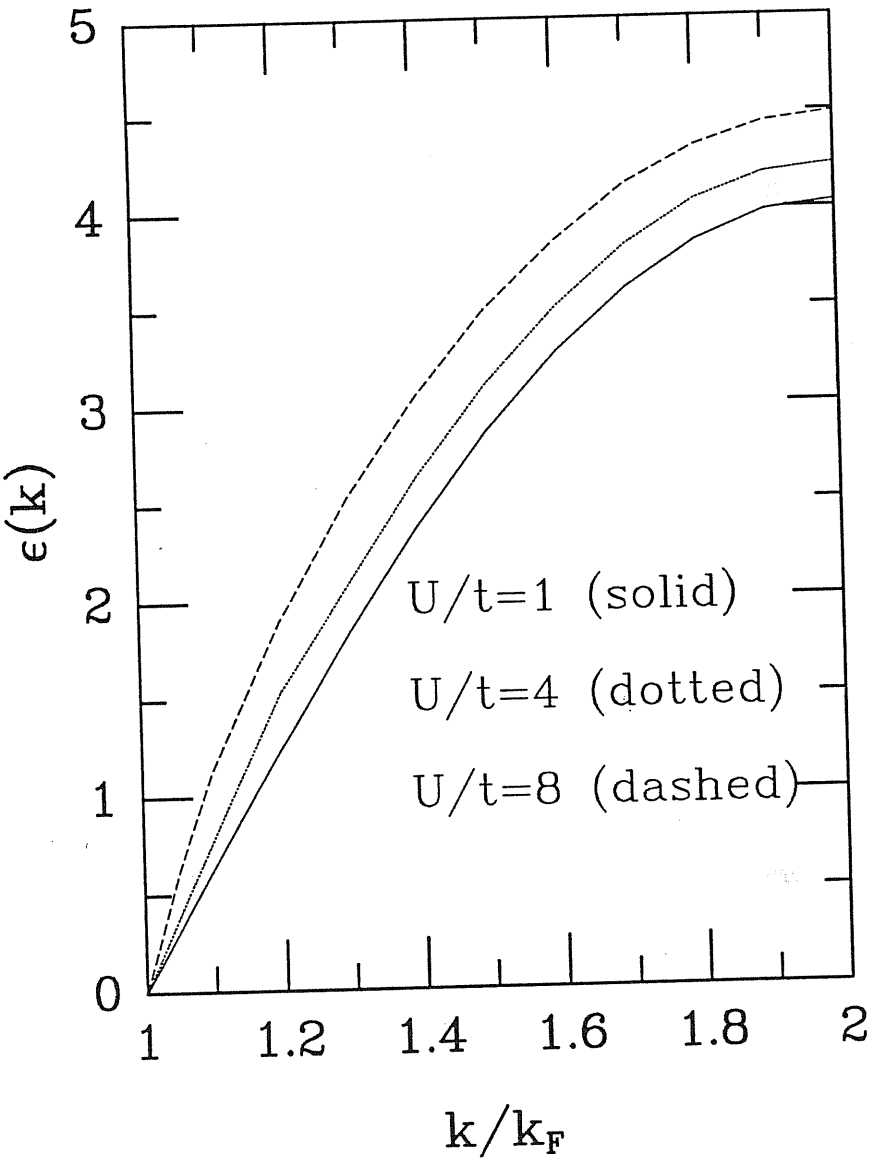


Figure 3.5: The single particle excitation spectrum for them Gutzwiller wave function at $\rho = 1$, as obtained by the FHNC/0. Hole excitations are identical, due to particle-hole symmetry.

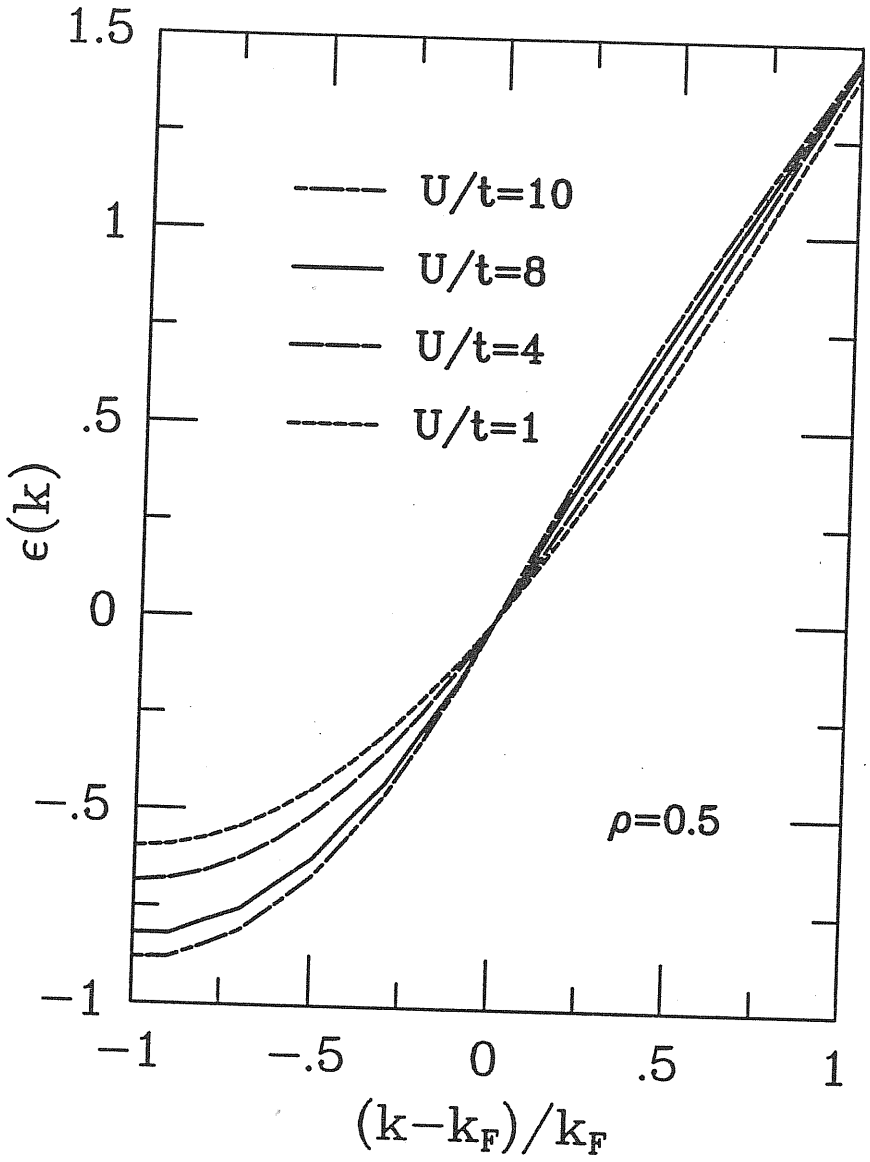


Figure 3.6: The single particle excitation spectrum for the Gutzwiller wave function at $\rho = 0.5$.

neighbor correlations (Jastrow type correlations).

$$f^J(x_{ij}) = \begin{cases} g & x_{ij} = 0 \\ g_1 & |x_{ij}| = a \\ 1 & otherwise \end{cases} \tag{3.6}$$

The calculation of the expectation value of the hamiltonian is of similar simplicity as for the Gutzwiller case. We have minimized total energy $E$ with respect to $g$ and $g_1$. The improvement of $E$ was found to be quite small, comparable with the accuracy of our calculation [23]. The energy expectation value has been found to be a very flat function of $g_1$ for $g_1$ around 1. Inclusion of second and higher neighboring site correlations yields corrections that site are even smaller, and totally negligible. These longer range correlations have however some minor effect on $n(k)$ as can be seen from Fig. 3.7.

On the basis of the above analysis it emerges quite clearly that the discrepancy between the Gutzwiller and Lieb and Wu result is not due to a poor choice of state independent two-body correlations. The importance of other correlations, particularly of the $e-d$ type will be discussed in the next Chapters.

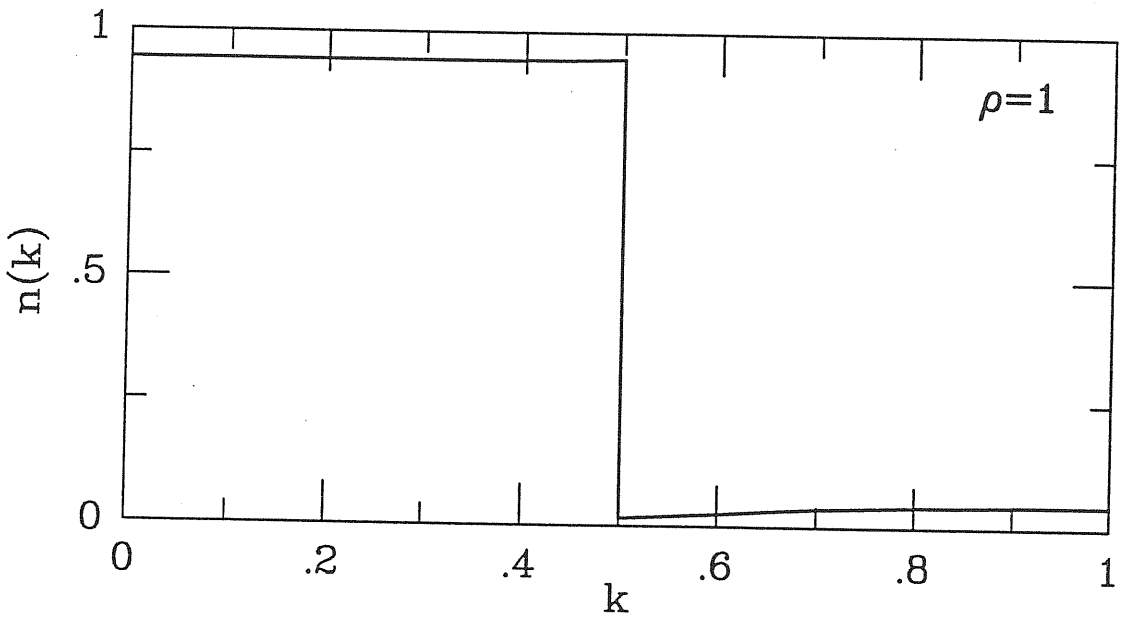


Figure 3.7: Momentum distribution function for Jastrow wave functions ($g_1 \neq 0$) compared with Gutzwiller ones ($g_1 = 0$).

# Chapter 4

# Four-particle ("quartet") implementation of e-d (charge-charge) correlations

## 4.1 The importance of the correlation

As shown in the previous Chapter, the FHNC/CBF realization of Gutzwiller correlations can be considered on the whole quite satisfactory. This success however does not cure the fact that Gutzwiller correlations are themselves basically unsatisfactory, as is well-known, on several accounts. A very good physical description of the differences of pure Gutzwiller correlations in the 1D Hubbard model can be found in a recent article by Fazekas and Penc [25]. The main missing ingredients, at least near half-filling ($\rho \approx 1$), are known to be the charge-charge correlations, particularly

the so called $e-d$ correlations, discussed originally by Kaplan, Horsch and Fulde [20], and later by many others [16][21]. Empty ($e$) and doubly occupied ($d$) sites, which the Gutzwiller wave function leaves mutually uncorrelated, prefer in the true ground state to sit on neighboring sites.

We can present the following qualitative *rationale*, due to Tosatti [29], of these correlations. At half-filling, where $e$ and $d$ are present in equal numbers, bound pairs are actually formed, with a binding energy equal to the insulating gap. Because of this, we can argue that $e-d$ correlations must fall exponentially with distance. The nature of the insulating ground state can be seen as "excitonic", i.e., it contains a "condensate" of $(ed)$ pairs. Away from half filling, say for $\rho < 1$, there is an excess of $e$ over $d$, and the final nature of the ground state is decided by a three-body scattering process, $e + (ed)$. The general belief that in this regime the 1D Hubbard model becomes a marginal conductor, that is, borderline between a metal and an insulator [3], could imply that, although the (ed) bound state is not destroyed, its binding energy must fall to zero. Hence, in this case long-range $e-d$ correlations will decrease only as a power law of relative distance.

Our task in this Chapter, is to build at least some of these important ed correlations into the present FHNC/CBF calculation scheme. Drawing heavily from previous experience on the same problem with different methods [20], we shall content ourselves with introducing nearest-neighbor correlations only. They are the simplest to implement, and they are also the most important in reducing the total energy. We are of course well aware, in doing this, that many other physically important aspects, such

as metallic versus insulating character, and Fermi liquid versus non-Fermi liquid behavior would also require a proper treatment of $long-range$ correlations, which at this stage we do not provide. Similarly to Fazekas and Penc [25], we prefer to take one step at a time, by demonstrating at this initial stage how the simpler short-range $ed$ correlations can be included. Extension to long-range correlations seems conceptually feasible, but is left for the future.

## 4.2 Four-particle correlations

In the present real space method, inclusion of nearest neighbor $e-d$ correlations involves a minimum of $four$ electron sites, (which we call a "quartet"). Calling $x = 0$ the coordinate of a doubly occupied site $d$, we start by assuming $r_1 = 0, r_2 = 0$. [Fig. 4.1]. Then, if a third electron, of coordinate $r_3$, occupies a first-neighbor site, $|r_3| = a$, we can require that no fourth-electron should be as close, i.e. $|r_4| \geq 2a$. If only configurations which obey this rule were included, the confinement of the $(ed)$ pair would be total. What we do, is to include the possibility to enhance (or depress) this type of configurations by taking as our new variational state

$$|\Psi >= QG|\Phi >, \tag{4.1}$$

where

$$Q = \begin{cases} \eta & \text{if } x_{12} = 0,\ x_{13} = a,\ x_{14} \neq 2a \\ 1 & \text{otherwise} \end{cases} \tag{4.2}$$

In calculating the pair distribution function and the one body density matrix the quartet correlations can be treated as 4-point bridge structures.

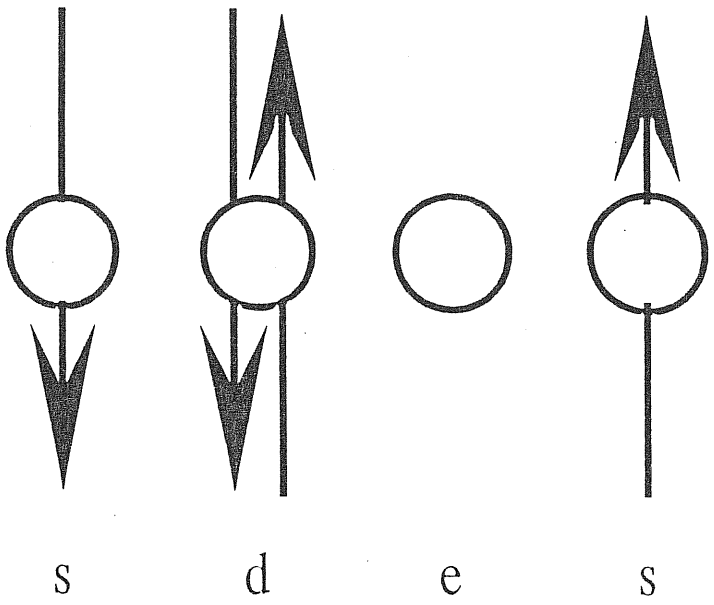


Figure 4.1: Example of $e - d$ configuartions in 1D lattice. $e$ refers to an empty site, $d$ a doubly occupied one, and $s$ for singly occupied sites. Such configurations are favored variationally in the CBF calculation.

Correspondingly, one has to calculate four functions $Q_{dd}, Q_{de}, Q_{ee}$, and $Q_{cc}$ related with the 4-point irreducible diagrams having the quartet correlations and the various bond dressed with the proper distribution functions. For example, the function $Q_{dd}$ is given by

$$\begin{aligned} Q_{dd}(x_{12}) &= \sum_{x_3,x_4} Q^2(x_1,x_2,x_3,x_4) \\ &\times \sum_i g_{\alpha_i}(x_{13}) g_{\beta_i}(x_{14}) g_{\gamma_i}(x_{23}) g_{\delta_i}(x_{24}) g_{\mu_i}(x_{34}) c_i \end{aligned} \tag{4.3}$$

where the second summation follows the same rule for the combinations of $g$'s as in $E^4_{dd}$ which is given in Table I in Appendix $B$, with the only difference that the bond $g_{dd}-1$ becomes here $g_{dd}$.

Similar expressions are found for $Q_{de}, Q_{ee}$ and $Q_{cc}$, which they refer to Tables II-IV. Each quartet function $Q_{ab}$ is then summed to the correspond bridge function $E_{ab}$ into the FHNC equations (2.21-25). The calculation of the density matrix is performed in an analogous way. The quartet functions $Q_{\xi d}, Q_{\xi e}, Q_{\xi cc}$ and $Q_\xi$ are respectively added to bridge functions $E_{\xi d}, E_{\xi e}, E_{\xi cc}$ and $E_\xi$ in the equations (2.30-32) and (2.34). They are given by one equation similar to (4.3) with $Q(x_1...x_N)$ in place of $Q^2(x_1...x_N)$. The $g$-combination follows Table V, VI, VII, and IX with $g_{\xi d}-1$, $g_{dd}-1$ substituted with $g_{\xi d}$, $g_{\xi d}$, respectively. There are no quartet function of the type $Q_{\xi\xi}$ and $Q_{\xi c\xi c}$.

The resulting FHNC equations turn out to be of the same complexity as in the case of the pure Jastrow model discussed in Chapter 3. More realistic quartet correlations, including also long-range correlations would not imply any extra real difficulty with respect to that employed here and given in Eq. (4.1). We also note that the introduction of quartet correlations leads

to a more rapid convergence process in the solution of the FHNC equations, and to a better fulfillment of the various sum rules discussed in Chapter 3.

## 4.3 Results and Discussion

In Fig. 3.3, we have shown the minimized total energy with the use of Quarlet/Jastrow correlations. For $U/t = 4$, the variational parameters $\eta$, $g_1$ and $g$ are found to be $-0.50, 0.80$ and $0.45$ for $\rho = 1$, $-0.45, 0.80$ and $0.45$ for $\rho = 0.8$ and $-0.45, 0.75$ and $0.45$ for $\rho = 0.6$, respectively.

The quartet correlations accounts for as much as 90% of the discrepancy between the results of the Gutzwiller model and the exact ground state energy, in qualitative accordance with the calculations of Ref. [25]. For example, for $U/t = 4, \rho = 1$, we have $E_{Gutzwiller}/N = -.521, E_{Q/Jastrow} = -.565$ compared with $E_{exact}/N = -.571$ [3]. The results for $< E > /Nt$ are reported together with the corresponding Gutzwiller evolution in Fig. 3.3 for various filling factors.

Another important indication of the fact that the quartet correlation improve the ground state wave function comes from the results obtained from the momentum distribution, which are shown in Fig. 4.4 and 4.5 for $\rho = 1$ and 0.8. The magnitude of the drop of $k = k_f$ is reduced, although not eliminated, by the inclusion of quartet correlations. In particular, $n(k)$ changes from increasing to decreasing just before $k_F$. This feature goes qualitatively in the right direction when one compares with numerically obtained $n(k)$ based on exact solution of the 1D Hubbard model [30].

In fact the inclusion of quartet leads to a decrease of $n(k)$ for $k < k_F$,

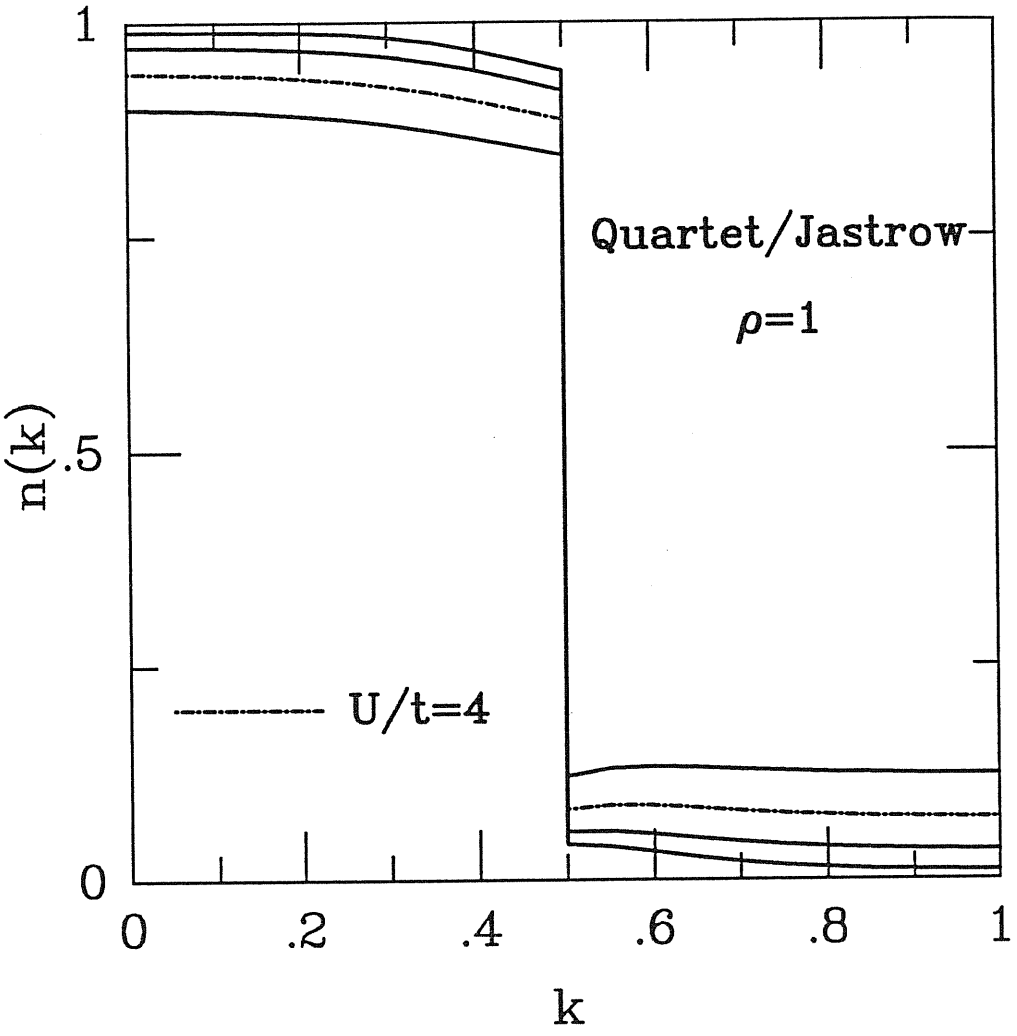


Figure 4.4: Momentum distribution function for the quarlet wave function at $\rho = 1$. Dashed line corresponds to the case $U/t = 4$, while solid line corresponds to the case $\eta = -0.50$, $g_1 = 0.80$, $g = 0.50, 0.40$ and $0.35$ respectively.

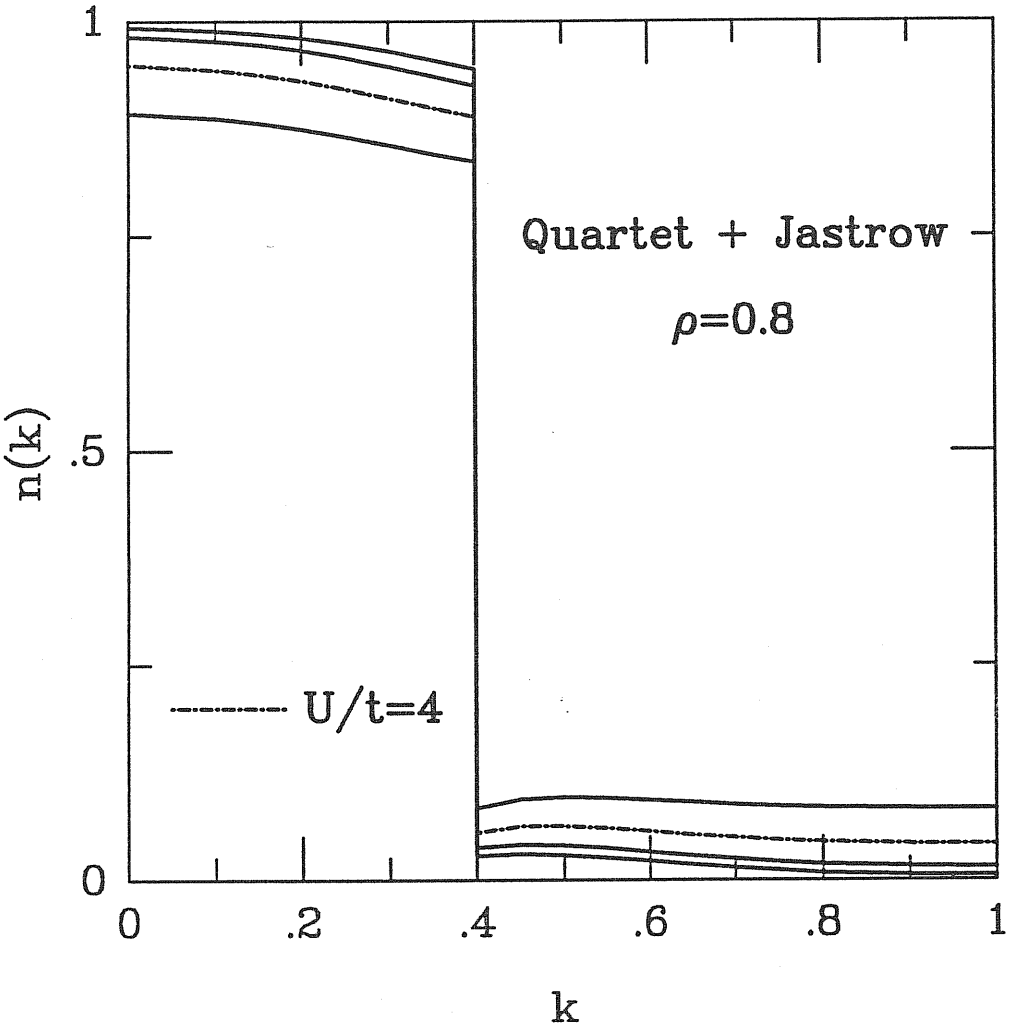


Figure 4.5: Momentum distribution function for the quarlet wave function at $\rho = 0.8$. Dashed line corresponds to the case $U/t = 4$, while solid line corresponds to the case $\eta = -0.50$, $g_1 = 0.80$, $g = 0.45, 0.40$ and $0.35$ respectively.

in accordance with the exact solution by Lieb and Wu.

# Chapter 5

# Spin correlations

## 5.1 State-dependent spin correlations

Spin dependent correlations modify the distributions of singlet and triplets with respect to that of the Slater determinant and are also suggested by the well-knowbn antiferromagnetic tendencies of the Hubbard model. Therefore it is interesting to study the effect of their inclusion on the energy. This has been accomplished by considering the correlation operator

$$G = G^J G^{SD} = S \prod_{i,j} (1 + \hat{\eta}_2(i,j)), \tag{5.1}$$

in the wave function $\Psi_0$ of Eq. (2.1). A correct FHNC treatment for such a correlation operator requires that chain, hyperchain and bridge diagrams are computed by taking care of all possible orderings of the $\hat{\eta}_2(i,j)$ correlations. The approximation, denoted as Single Operator Chain (SOC) [13], includes the leading diagrams with links corresponding to spin correlations. It has been applied to study nuclear matter and more recently,

an improved version of SOC has been successfully used in liquid $^3$He [12], where spin-dependent correlations are crucial. Unfortunately, at present, it is not clear how to go beyond the FHNC/SOC scheme of Ref. [34] which may be necessary to study the Hubbard hamiltonian. An interesting way to overcome such a difficulty would be to consider a $G^{SD}$ of the so-called independent cluster form

$$G_{IC(M)} = 1+\sum_{ij} \hat{\eta}_2(i,j)+\sum_{ijk} \hat{\eta}_M(i,j,k)+...+ \sum_{i,j\neq l,m} \hat{\eta}_2(i,j)\hat{\eta}_2(l,m)+..., \quad (5.2)$$

where the cluster correlation $\eta$'s appearing in each sum have no common indices, and $M$ denotes the largest cluster included. An exact FHNC treatment can be derived for each $M$, which is free of the "commutator terms". The case $M = 2$ has already been developed to study liquid $^3$He [12] and work to include three-body clusters $\hat{\eta}_3(i,j,k)$ are in progress.

## 5.2 LCE method

In the present work we limit our analysis to very weak spin correlation functions $\eta(r_{ij})$. Unlike $^3He$, weak spin correlations are, as it turns out, quite appropriate for the Hubbard model. Since they also have a very short range nature, it is expected that they can be well accounted for by the second order of the power series cluster expansion [9], namely by retaining all the cluster diagrams having at most two $\eta(i,j)$ correlations. This approximation allows us to include correctly all the orderings in the diagrams considered. The quadratic terms in $\eta$ are necessary in order to determine a minimum in the expectation value of the hamiltonian with respect to the

variational parameter of $\eta(i,j)$.

In this calculation we limit ourselves to consider the simplest variational choices for both the Jastrow correlation $f(r_{ij})$ and the spin correlation function $\eta(r_{ij})$, namely

$$f(r_{ij}) = \exp\{\frac{1}{2}\alpha\delta_{ij}\}, \tag{5.3}$$

$$1 + \hat{\eta}(i,j) = \exp\{\frac{1}{2}\eta\delta_{|i-j|,1}\vec{\sigma}_i\vec{\sigma}_j\}. \tag{5.4}$$

On site spin-correlations are already included in the Gutzwiller ansatz (5.3), since two electrons in the same site must in a singlet state only. It follows that the simplest interesting variational choice for $\eta(i,j)$ is to correlate the first neighbor sites as in Eq. (5.4).

The pair correlation function at $x_{ij} = 0$ is given by

$$g(0) = \frac{2}{A\rho} < \sum_{i<j} \delta_{ij} >, \tag{5.5}$$

where $< >$ denotes the expectation value on $G\Phi$. The zeroth order term is $1/2$. First order terms are obtained from the equations

$$g^{(1)}(0) = \alpha\frac{d}{d\alpha}g(0)\Big|_{\alpha,\eta=0} + \eta\frac{d}{d\eta}g(0)\Big|_{\alpha,\eta=0}, \tag{5.6}$$

whose evaluation requires that of two- three- and four-body uncorrelated distribution functions. In fact,

$$\begin{aligned}\frac{d}{d\alpha}g^{(0)}|_{\alpha,\eta=0} &= \frac{2}{A\rho}\{< \sum \delta_{ij}\delta_{jm} >_\Phi - < \sum \delta_{ij} >_\Phi < \sum \delta_{jm} >_\Phi\} \\ &= \frac{2}{A\rho}\sum_{connected} < \sum \delta_{ij}\delta_{jm} >_\Phi \end{aligned} \tag{5.7}$$

where $< >_\Phi$ denotes the expectation value on the uncorrelated wave function $\Phi$ and the last sum is limited to the connected diagrams only. The

two-, three- and four-body distribution functions are required to calculate the terms arising from $(ij)$ and $(lm)$, having both, one and no common indices respectively. An analogous expression holds for the spectrum

$$\frac{d}{d\eta}g(0)\Big|_{\alpha,\eta=0} = \frac{d}{d\eta}\sum_{connected} < \delta_{ij}\delta_{|j-m|,1}\vec{\sigma}_l\vec{\sigma}_m >_\Phi \tag{5.8}$$

Here, the two body terms vanish, since $\delta_{ij}\delta_{|i-j|,1} = 0$. One can easily verify that

$$g^{(1)}(0) = \frac{\alpha}{6} + \frac{6\eta}{\pi^2} \tag{5.9}$$

Similarly, the quadratic terms are provided by the equation

$$\begin{aligned} g^{(2)}(0) &= \frac{1}{2}\alpha^2\frac{d^2}{d\alpha^2}g(0)\Big|_{\alpha,\eta=0} + \frac{1}{2}\eta^2\frac{d^2}{d\eta^2}g(0)\Big|_{\alpha,\eta=0} + \frac{1}{2}\eta\alpha\frac{d^2}{d\alpha d\eta}g(0)\,|_{\alpha,\eta=0} \\ &= \frac{1}{A\rho} < \sum_{connected} \delta_{ij}(\alpha\delta_{lm} + \eta\delta_{|l-m|,1})(\alpha\delta_{np} + \eta\delta_{|n-p|,1}) >_\Phi \end{aligned} \tag{5.10}$$

They turn out to be

$$g^{(2)}(0) = \eta^2(-\frac{3}{4} + \frac{39}{4\pi^2} + \frac{24}{\pi^4}) + \frac{6\alpha\eta}{\pi^2}(-1 + \frac{8}{\pi^4}). \tag{5.11}$$

A completely similar procedure can be used to evaluate the zeroth, first and second order terms of the density matrix which is needed to compute the kinetic energy expectation value. The zeroth order term gives $2/\pi$ and it is found that first order terms in both $\alpha$ and $\eta$ vanish. The net result for the second order terms is given by

$$n^{(2)}(0) = -2\alpha^2(\frac{1}{16} + \frac{1}{4\pi^2}) - \frac{2\eta^2}{\pi}(\frac{27}{16} + \frac{20}{3\pi^2}) - \frac{2\alpha\eta}{\pi}(\frac{2}{\pi^2} + \frac{3}{8}). \tag{5.12}$$

## 5.3 Discussion

If we set $\eta = 0$ we recover the LCE expression [9]. In this case the minimum of $E/t$ for $U/t = 4$ is -0.521 with $\alpha = -1.49$, whereas for the full

Table I:

Energies calculated by second order power series expansion with and without nearest-neighbour spin correlations.

| $U/t$ | $E_{\eta=0}/N$ | $E_{\eta\neq 0}/N$ |
|---|---|---|
| 1 | -1.038 | -1.039 |
| 2 | -0.835 | -0.836 |
| 4 | -0.522 | -0.528 |

expression the minimum is $-0.528$ with $\alpha = -1.366$ and $\eta = 0.044$. These results strongly indicate that short range spin-dependent correlations do not give a substantial contribution in the 1D case, as was anticipated. Therefore a full calculation with the SOC scheme (or beyond) seems not to be necessary here. Table II shows the equation of state for different value of $U/t$ calculated with second order power series expansion with or without spin correlations.

# Chapter 6

# Correlated BCS function

## 6.1 The motivation

All correlations which we have implemented so far consist of one projected or another (Gutzwiller, Jastrow, *ed*, spin-spin) acting on the bare Slater Determinant $|Fermi\ Sea>$. Mainly due to that, the resulting system turns out to be "Fermi liquid" like. That is the underlying single-particle Green's function retains a non-zero pole residue $Z$

$$G_{k\epsilon} = \frac{Z}{\epsilon - e_k + i\delta} + nonpole\ terms \tag{6.1}$$

which in turn is reflected by a finite jump of $n(k)$ at $k = k_F$.

As was repeatedly stated, it is of course well known that in reality this particular detail is wrong in the 1D Hubbard model, which is in fact a true insulator for $\rho = 1$ [3], and only a marginal metal, with $Z = 0$ at all other fillings [4]. We notice that, for example, the ed correlation results of Chapter 4, yield a ground state energy which is already very

close to the exact result, and yet, the Fermi jump is still quite large in that approximations. Implicitly, this demonstrates that departure from Fermi liquid behavior, at least for $\rho \neq 1$, is probably connected with an extremely small and delicate energetic improvement.

Nevertheless, this Fermi-liquid issue is of great conceptual importance, as well as a subject of intense debate in the 2D case [8]. It is therefore of interest to investigate at least one class of trial wave functions which by construction, do not have a Fermi surface. The simplest such state is a band antiferromagnetic ground state with spatial periodicity $\pi/k_F$, which is usually referred to as a Spin Density Wave (SDW) state. In that case, the uncorrelated state $|\Phi>$ is just a magnetic band insulator, at any filling, and the Fermi Surface is trivially destroyed by single-particle magnetic Bragg scattering. A CBF calculation starting with a SDW uncorrelated state will be presented in the next chapter.

A second, more challenging type of wave function without a Fermi jump is a BCS state. It was shown a long time ago by Fantoni [39] that, in spite of its not being a single Slater determinant, a BCS function can usefully be employed as the starting point for a CBF calculation [35].

Energetically, we can surmise at the outset that BCS correlations might not be favorable in the 1D repulsive Hubbard model. The Tomonaga mapping, for example [36], indicates that the pairing susceptibility does not diverge in this regime.

Our main reason for carrying out a correlated BCS calculation all the same is thus largely "educational". In the 2D, $U = \infty$ case (where the physics is different), Anderson has indicated that some kind of Gutzwiller

projected BCS state maybe a reasonable representative for his RVB state. In fact in 2D, there are indications that such a state with a d-wave pairing function has quite a good energy [37][38].

## 6.2 Correlated BCS theory

Since $|BCS>$ is not an eigenstate of the particle number operator $\hat{N}$, we need to write $G$ in the form of a second quantized operator [39]

$$|\Psi_{BCS}>=\hat{G}|BCS> \tag{6.2}$$

with

$$|BCS>=\prod_{\mathbf{k}}(u_{\mathbf{k}}+v_{\mathbf{k}}c^{\dagger}_{\mathbf{k}\uparrow}c^{\dagger}_{-\mathbf{k}\downarrow})|0>, \tag{6.3}$$

where the BCS amplitude $u_{\mathbf{k}}$ and $v_{\mathbf{k}}$ are variational functions subjected to the normalization condition $u^2_{\mathbf{k}}+v^2_{\mathbf{k}}=1$. The correlation operator $\hat{G}$ is defined through the following equation

$$|\Psi_{BCS}>=\sum_{L}\sum_{m_L}\hat{G}_L|\Phi^{(m_L)}_L><\Phi^{(m_L)}_L|BCS>, \tag{6.4}$$

where the label $m_L$ specifies a set of $L$ single particle states. In coordinate representation $\hat{G}_L|\Phi^{(m_L)}_L>$ is given by

$$<x_1...x_L|\hat{G}_L|\Phi^{(m_L)}_L>=G(1,...L)A\{\Psi_{m_1}...\Psi_{m_L}\}, \tag{6.5}$$

where each index $m_i$ denotes both the momentum $\vec{k}$ and the spin projection $\sigma$ of the state. In this work we limit our attention to consider operator $G(1,...L)$ of the Jastrow form, namely $G(1,...L)=\prod_{i>j=1,L}f(r_{ij})$. By construction $|\Psi_{BCS}>$ has an off diagonal long range order.

The FHNC equations to calculate the pair distribution function and the density matrix are given in ref. [14] for a Fermi liquid. The modifications needed to apply these equations to the present 1D lattice calculation are straightforward and follow the procedure discussed in the previous Chapters. The correspond solution of these equations is of the same amount of simplicity as in the Fermi sea case.

The density $\rho_0$ of the uncorrelated $|BCS>$ state vector, given by

$$\rho_0 = \frac{2}{N}\sum_k v^2(k), \tag{6.6}$$

is not the same as the density $\rho$ of $|\Psi_{BCS}>$. It follows that $\rho_0$ has to be considered as a variational parameter of the theory, whereas $\rho$ results from the solution of FHNC equations. In fact $\rho = c\rho_0$ appears in the FHNC diagrams as a vertex correction and $c$ has to be calculated self-consistently together with the other FHNC quantities $N_{ab}, X_{ab}$ and $E_{ab}$.

## 6.3 Results and Discussion

Fig. 6.1 summarizes our calculated CBF/FHNC ground state energies for the Gutzwiller-correlated BCS state of the 1D Hubbard model.

Clearly, the introduction of a BCS order parameter is not energetically favorable, as expected from the previous discussion. In essence (see Fig. 6.2) the BCS pairing increases the double occupancy significantly, without yielding a kinetic energy gain sufficient to compensate. Writing the total energy in the form

$$E(\Delta) = E_0 + \chi\Delta^2/2 \tag{6.7}$$

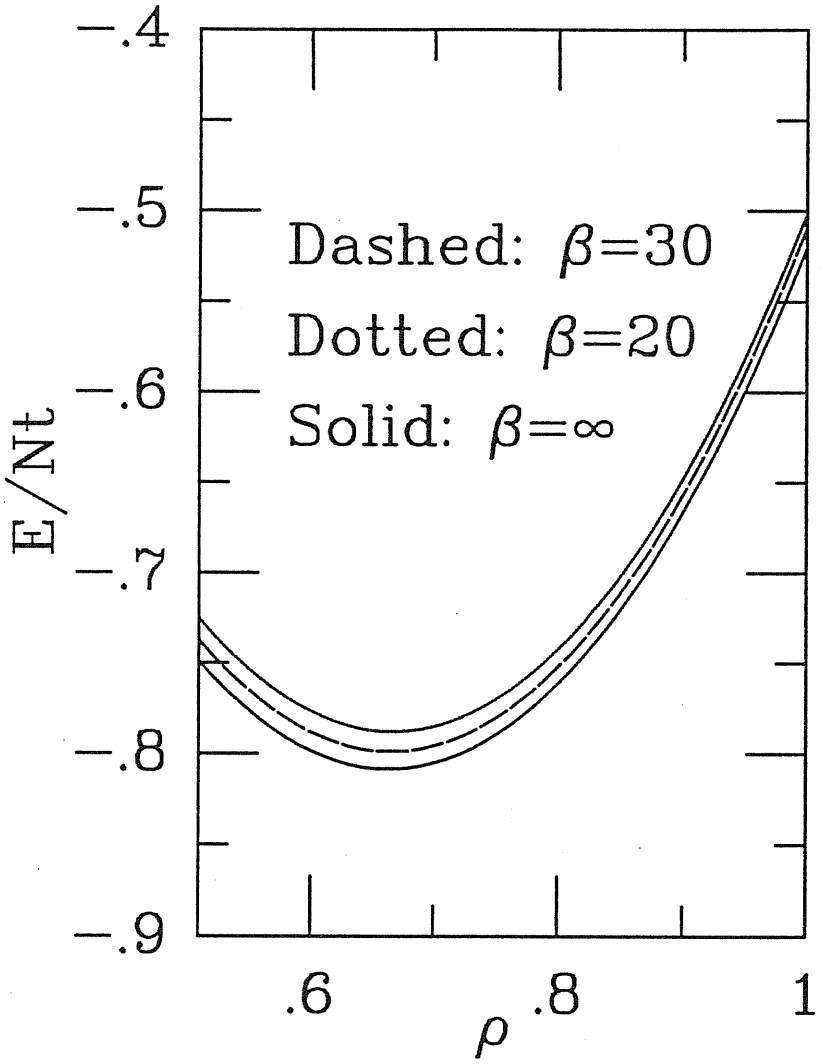


Figure 6.1: Ground state energies for the Gutzwiller-correlated BCS state of the 1D Hubbard model. The variational functional $u(k)$ are chosen of the form $u(k) = 1/(1 + exp(\beta(\epsilon_k - \mu)))$ with $\beta, \mu$ being variational parameters. At $\rho = 1$ (half filling), $\mu = 0$ and $\mu$ is used for the control of the initial input for $\rho_0$.

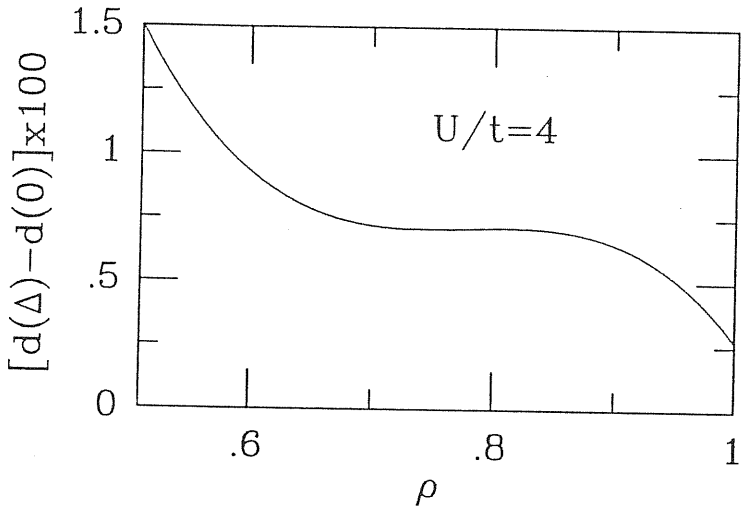


Figure 6.2: The increase of the double occupancy by introducing BCS pairing.

we can extract the pairing susceptibility as a function of filling. That susceptibility is shown in Fig. 6.3.

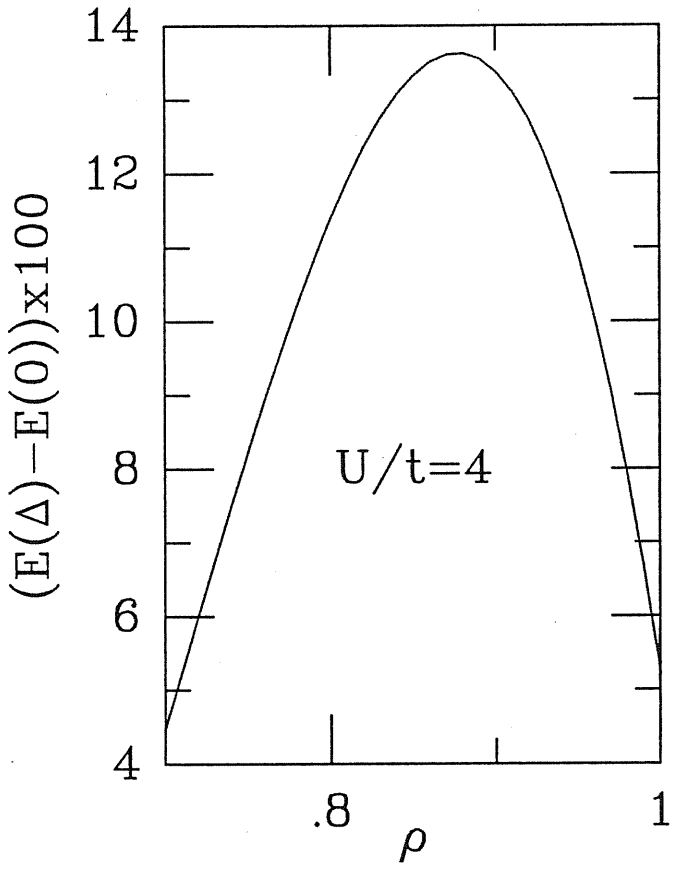


Figure 6.3: Pairing susceptibility as a function of filling.

# Chapter 7

# Correlated Spin-Density-Wave Theory

## 7.1 Introduction

In previous chapters, we demonstrated that the CBF/FHNC method is in fact useful in the application to the Hubbard model. As a continuation of the previous work, the CBF method is extended to include the antiferromagnetic long-range order. The theory is based on the Jastrow-type correlation factor and its effect is taken into account by the FHNC procedure. An application is made to the half-filled-band case of one dimensional lattice. Notice that the nesting condition is completely satisfied for the half-filled band in the system. Therefore the antifferromagnetism tends to be realized easily here. In fact, the lowest energy within the paramagnetic Gutzwiller wave function is higher than the antiferromagnetic

Hartree-Fock solution in strong coupling regime [9][31].

This chapter is arranged as follows. In section 7.2, we develop the correlated SDW theory. The results are presented in section 7.3, and in section 7.4, summary and supplementary discussion are given.

## 7.2 Model and Wave Function

By transforming Eq. (1.1) to momentum space, the Hubbard hamiltonian $H$ can be expressed as

$$\begin{aligned} H &= \sum_{k,\sigma} \epsilon_k c^\dagger_{k\sigma} c_{k\sigma} \\ &+ \frac{U}{2}\frac{1}{N}\sum_{kk'q}\sum_{\alpha\beta} c^\dagger_{k',\alpha} c^\dagger_{-k'+q,\beta} c_{-k+q,\beta} c_{k\alpha}, \end{aligned} \tag{7.1}$$

where $\epsilon_k = -2tcos(k_x)$ (for 1D), $\epsilon_k = -2t(cos(k_x)+cos(k_y))$ (for 2D square lattice), $\alpha, \beta$ are the indices for spin quantization along the $z$ direction, and $N$ is the total number of sites.

Assume a SDW whose mean field is polarized in the $z$ direction

$$\sum_{k\alpha} < SDW | c^\dagger_{k+Q,\alpha} c_{k\alpha} sgn(\alpha) | SDW >= NS, \tag{7.2}$$

where the variational parameter $S$ will be determined later by a self-consistency condition. In the presence of this mean field, the Hartree-Fock factorization can be worked out with the $i,j$ element of the Slater determinant of the ground state (with the Hartree-Fock-type antiferromagnetic order):

$$\varphi_{k\sigma}(r_i) = (u(k)e^{ikr_i} + sgn(\sigma)v(k)e^{i(k+Q)r_i})\xi_\sigma(i) \tag{7.3}$$

for $k < k_F$;

$$\varphi_k(r_i) = (v(k)e^{ikr_i} - sgn(\sigma)u(k)e^{i(k+Q)r_i})\xi_\sigma(i) \tag{7.4}$$

for $k > k_F$, where

$$\begin{aligned} u_k &= [\frac{1}{2}[1 + \frac{\epsilon_k}{E_k}]]^{1/2}, \\ v_k &= [\frac{1}{2}[1 - \frac{\epsilon_k}{E_k}]]^{1/2}, \\ E_k &= (\epsilon_k^2 + \Delta^2)^{1/2}, \\ \Delta &= -\frac{US}{2}, \end{aligned} \tag{7.5}$$

and sgn($\sigma$) takes either +1 or -1 according as $\sigma = \uparrow$ or $\downarrow$; and $\mathbf{Q}$ is the wavevector characterizing the extra periodicity due to the antiferromagnetic ordering. In principle, $\mathbf{Q}$ could be determined so as to minimize the energy. Here, we do, however, make no attempt to deal with this problem. Instead we choose a simple two-sublattice antiferromagnetic structure, and $\mathbf{Q}$ is then defined by the condition that

$$e^{i\mathbf{Q}\mathbf{t}} = -1 \tag{7.6}$$

for all translations t which transform one sublattice into the other. Thus $e^{i\mathbf{Q}\mathbf{r_i}}$ is equal to +1 in one sublattice and -1 in the other, then in practice $\mathbf{Q}$ is $\pi$, or $(\pi, \pi)$ for 1D chain or 2D square lattice.

The self-consistency condition determining the gap parameter $\Delta$ can be obtained as [9]

$$SN = -4\sum_k{}' \frac{\Delta}{2E_k} = -\frac{2\Delta}{U}N. \tag{7.7}$$

In this formulation $\Delta$ is a variational parameter to be determined so as to minimize the total energy. The ordinary (paramagnetic) CBF is a special

case of this function, i.e., $\Delta = 0$, since eq. (7.4-7.5) is reduced then to the Slater determinant of free electrons.

The one-body density in this case is given by:

$$\begin{aligned} \rho &= \frac{1}{N}\sum_{k,\sigma}\varphi^*_{k\sigma}(1)\varphi_{k\sigma}(1) \\ &= \frac{1}{N}\sum_{k,\sigma}\{u^2(k)+v^2(k)\} = \frac{A}{N}, \end{aligned} \tag{7.8}$$

and the uncorrelated two-body density matrix is given by:

$$\begin{aligned} \rho(1,2) &= \frac{1}{N}\sum_{k,\sigma}\varphi^*_{k\sigma}(1)\varphi_{k\sigma}(2) \\ &= \sum_{\sigma}\xi^*_{\sigma}(1)\xi_{\sigma}(2)[(l_u(r_{12}) + e^{iQr_1}l_v(r_{12})sgn(\sigma)] \\ &= \sum_{\sigma}\xi^*_{\sigma}(1)\xi_{\sigma}(2)\hat{\rho}_{\sigma}(r_{12}) \end{aligned} \tag{7.9}$$

where

$$l_u = \frac{1}{N}\sum_{k<k_F}\{u^2(k)e^{-ikr_{12}} + v^2(k)e^{-i(k+Q)r_{12}}\}, \tag{7.10}$$

$$l_v = \frac{1}{N}\sum_{k<k_F}u(k)v(k)e^{-ikr_{12}}(1+cos(Qr_{12})). \tag{7.11}$$

The FHNC equations remain unchanged for $dd$, $de$ and $ee$ functions, while due to the broken of translational invariance, it is convenient to consider $\rho$, and consequently $X_{cc}$, $N_{cc}$ as two component vectors:

$$\hat{\rho}_{\sigma} = \begin{pmatrix} l_u \\ l_v \end{pmatrix}; \hat{X}_{cc} = \begin{pmatrix} X^u_{cc} \\ X^v_{cc} \end{pmatrix}; \hat{N}_{cc} = \begin{pmatrix} N^u_{cc} \\ N^v_{cc} \end{pmatrix} \tag{7.12}$$

The convolution integral is then given by:

$$Z = (G|F) \tag{7.13}$$

with

$$Z_u = \int dr_3 F_u(r_{13}) G_u(r_{32}) + \int dr_3 F_v(r_{13}) cos(Q r_{13}) G_v(r_{32}),$$
$$Z_v = \int dr_3 F_v(r_{13}) G_u(r_{32}) + \int dr_3 F_u(r_{13}) cos(Q r_{13}) G_v(r_{32}). \quad (7.14)$$

The parallel connections between vector quantities is given by (note that these parallel connections imply also spin summation):

$$\hat{F}_{12} \bullet \hat{G}_{12} = Z_{12} = 2F_u(12)G_u(12) + 2cos(Qr_{12})F_u(12)G_v(12) \quad (7.15)$$

where the factor of 2 is due to spin summation. Therefore, the parallel connection of two vector quantities is a scalar quantity. The parallel connection of a scalar quantity with a vector one $\hat{A}$ is a vector quantity with components obtained by multiplying the scalar quantity with the $A_u$ and $A_v$ respectively.

$$F_{12}\hat{G}_{12} = \hat{Z}_{12} Z^u_{12} = F_{12} G^u_{12}; \qquad Z^v_{12} = F_{12} G^v_{12} \quad (7.16)$$

It is easy to verify that the convolution between two $l$ functions satisfying the following relation:

$$\int d3\rho(1,3)\rho(3,2) = \rho(1,2) \quad (7.17)$$

with such defined convolution integral. By using the above rules the FHNC equations for the correlated SDW follow in a straightforward manner. We have found [32] that the convolution integral Eq. (7.15) can be treated conveniently by the introduction of a matrix representation distinguish between translations from $A$ to $A$, $A$ to $B$, $B$ to $A$ and $B$ to $B$ for $A$ and $B$-type sublattices.

The convolution integral Eq. (2.15) is not symmetrical, i.e. $(F|G) \neq (G|F)$. Hence the cancellation process of the conventional FHNC equations does not occur here. It follows that the $cc$ equations has to be modified in the form:

$$\hat{N}_{cc} = (\hat{X}_{cc} + \hat{N}_{cc} - \hat{\rho}|\hat{X}_{cc} - (\hat{X}_{cc}|\hat{\rho})) - (\hat{X}_{cc}|\hat{\rho}). \tag{7.18}$$

This equation reduces to the conventional FHNC equation (Eq. (2.24)) when $l_v = 0$. The convolution is done between vector quantities in the way discussed previously, and one should always take care of the ordering in the practical calculations.

Similarly, the equations for $X_{\alpha\beta}$ are formally unchanged. The only care is to calculate correctly the products between vector quantities and of a scalar with a vector quantity (in $X_{ee}$ and $X_{cc}$).

A completely similar treatment has to be used to compute the correlated density matrix and the momentum distribution function. In order to take care of the ordering, the equations for $N_{\xi cc}$ and $N_{\xi c\xi c}$ are modified in the following form:

$$\begin{aligned} N_{\xi c\xi c}(r_{11'}) &= N^{\rho}_{\xi cc}(r_{11'}) + \rho(r_{11'}) + \rho \sum_k \{N^{x}_{\xi cc}(r_{1k}) X_{\xi cc}(r_{k1'}) \\ &+ N^{\rho}_{\xi cc}(r_{1k})(X_{\xi cc}(r_{k1'}) - X_{cc}(r_{k1'})) + X_{\xi cc}(r_{1k}) N^{\rho}(r_{k1'})\}, \end{aligned} \tag{7.19}$$

where

$$N^{\rho}_{\xi cc} = -\rho + (N_{\xi cc}|X_{\xi cc} - (X_{\xi cc}|\rho)), \tag{7.20}$$

and

$$N^{x}_{\xi cc} = X_{\xi cc} - (X_{\xi cc}|\rho) + (N^{x}_{\xi cc}|X_{\xi cc} - (X_{\xi cc}|\rho)). \tag{7.21}$$

## 7.3 Results (preliminary)

We present first FHNC/0 calculations for the 1D chain with the periodic boundary condition. The energy expectation value for various values of variational parameters are calculated. The minimum of the energy is searched for in the way in the $\Delta - g$ plane as discussed in Ref. [9]. For $U/t = 4$ the lowest energy is found to be -.526 at $\Delta = 0.27$ and $g = 0.5$. The location of the minimum is in an excellent agreement with the Variational Monte Carlo calculations based on the same wave function [9]. The total energy is slightly higher, but overall agreement is fairly good. The inclusion of elementary diagrams are expected to reach the better agreement, especially at small $U/t$ region.

The antiferromagnetic Gutzwiller wave function (AFGF) includes the original paramagnetic Gutzwiller function as well as the HF solution as a special case. The energy energy minimum within the paramagnetic Gutzwiller function, -.518, is lowered further by about 0.01 with the AFGF. Clearly the AFGF energy is lower than the HF theory as expected. For higher $U/t$ values, the correlation energy is found rather small, in agreement to the variational Monte Carlo calculations [9], indicating that the SDW is a better uncorrelated wave function at half filling. In Fig. 7.1 we show the calculated momentum distribution function for $U/t = 4$.

The extension of the present calculation to other densities, to more complicated correlation functions, and to the higher dimensions is straightforward. We are in progress of further calculations and the results will be presented elsewhere [32].

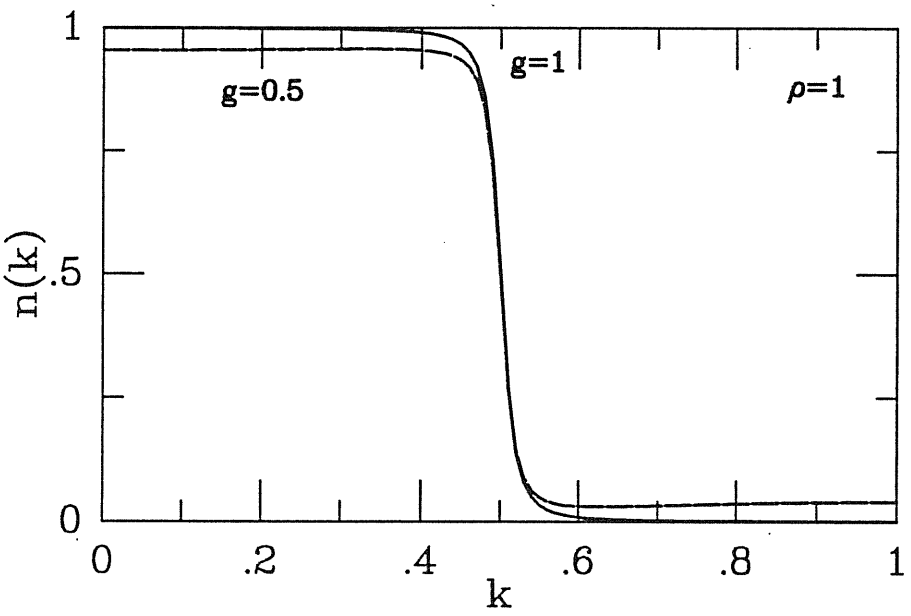


Figure 7.1: Momentum distribution function calculated by the correlated SDW theory for $U/t = 4, \rho = 1$.

## 7.4 Conclusions

In this Chapter we have developed the correlated SDW theory. We have chosen 1D Hubbard model as a test case. The Antiferromagnetic state is always stabilized for $U/t > 0$ and its energy stays lower than those of both the paramagnetic GF and the Hartree-Fock theory at half filling. Fast convergence has been found in the simulations for all $U/t$ values, especially for large $U/t$ ones. It should emphasized that the present method can go beyond the Gutzwiller wave function very easily, and the inclusion of Jastrow, four-body correlations is expected to give interesting results. Clearly there is still a great future potential in this method. New types of variational wave functions are being investigated. The direct physical nature of variational wave functions is readily allow for refinements. Altogether it is clear that variational wave functions will continue to be an extremely helpful theoretical too with excellent aspects, and it is interesting to apply the present CBF method to overcome the limitations imposed by working with small, finite systems.

# Chapter 8

# Overall discussion and conclusions

In this thesis, we have presented a first application of the CBF/FHNC methods to electrons on a lattice, for the particular case of the 1D Hubbard model.

Following the general formulation of Chapter 2, we have presented results for several different types of correlations, namely Gutzwiller, Jastrow, $e-d$ pairing, spin-spin, BCS and SDW correlations. The Gutzwiller results turn out to give energies and a momentum distribution which are quite close to the exact Gutzwiller calculations of Vollhardt and collaborators [16].

The Jastrow correlations, which generalize the Gutzwiller "on-site" approximation in allowing first-neighbor electron-electron correlations, is found to to provide only a negligibly small improvement over Gutzwiller. On the contrary, the introduction of first-neighbor correlations between an empty

(e) and doubly occupied (d) state does yield a dramatic energy improvement. At $\nu = 1, U = 4$ for example, the final result is only $\sim 1\%$ away from the exact Lieb-Wu result., while Gutzwiller is still $\sim 10\%$ above. The importance of attractive ed correlations was of course previous known [20][21], and has been very recently emphasized by Fazekas [25]. Our practical implementation of the ed correlations is technically interesting , and involves four-electron ("quartet") correlations.

Another type of correlations which is in principle present is first-neighbor spin-spin correlations. In the paramagnetic state, these correlations turn out to be weak, and their effect on the energy is marginal. For this reason, we have restricted ourselves to an analytic lowest order linked-cluster expansion, which yields a $< 1\%$-sized effect only.

The present method is applicable when the "uncorrelated" function is not a Slater determinant. As a demonstration of that, we have performed a Gutzwiller/BCS calculation, which turns out to be of similar difficulty as those based on a Slater determinant. Of course in this case there is no energy gain at all. We extract a BCS susceptibility which is new, as far as we can see. Finally, we have implemented Gutzwiller correlations on an antiferromagnetic SDW state. In this case too the energies is quite good, especially at half filling ($\rho = 1$).

It should be again clearly stressed that a great many of the subtleties of the 1D Hubbard model are not tackled at all by the present calculation. As any variational method, the trial wave function correlations, to be injected by hand, totally prejudice the outcome in this respect. The main "subtlety", i.e. non-Fermi liquid behavior has been deliberately ignored at

this stage.

With this provision in mind, the results of the present calculations can be defined very satisfactory. The method works well, and implementation is simple enough. However, convergence of the elementary diagram expansion is slow, probably due to the pathological nature of the on-site repulsion.

We believe that the present calculations demonstrate the potential usefulness of the CBF/FHNC methods for strongly correlated electrons on a lattice. Future applications to the Hubbard model in 2 and especially in 3 dimensions, as well as to more complicated models are now being considered.

# APPENDIX A

In this appendix, we introduce some terminology for diagrams used in CBF/FHNC method.

An $i-j$ subdiagram is a part of a diagram which is only connected with the rest of the diagram by means of the points $i$ and $j$.

A subdiagram is called *composite* if it is composed by two or more $i-j$ subdiagrams which form *parallel*, independent connections between the points $i$ and $j$.

Any $i-j$ subdiagram is either *nodal* or *nonnodal*. A subdiagram is nodal if it has one or more nodes, a node being an internal point through which any path joining the points $i$ and $j$ must pass. By definition, a composite subdiagram is nonnodal.

A subdiagram which is neither nodal nor composite is called *elementary* (bridge diagram).

A *basic* subdiagram is bridge diagram which has not any $i-j$ subdiagrams larger than the single bonds employed to construct subdiagrams (namely $\rho(k_F r_{km})$, $\rho^2(k_F r_{km})$, $h(r_{km})$, $h(r_{km})\rho(k_F r_{rm})$ and $h(r_{km})\rho^2(k_F r_{rm})$).

Examples of composite, nodal and elementary subdiagrams are shown in fig. 7.

Any $i-j$ subdiagram $\Gamma(i,j)$ may be also classified, by looking at the type of correlation lines reaching the points $i$ and $j$, in the following way:

$\Gamma_{dd}(i,j)$ if both the points $i$ and $j$ are not reached by statistical lines ($dd$=dynamical, dynamical),

$\Gamma_{de}(i,j)$ if point $i$ is not reached by statistical lines, whilst point $j$ is a

common extremity of two statistical lines ($de$=dynamical, exchange),

$\Gamma_{ee}(i,j)$ if both the points $i$ and $j$ are both reached by statistical lines ($ee$=exchange, exchange),

$\Gamma_{cc}(i,j)$ if both the points $i$ and $j$ are both reached by one statistical line ($cc$=cyclic, cyclic), namely are extremities of an exchange loop.

Starting from some given subdiagrams it is possible to construct other more involved subdiagrams by parallel connection or superposition of them. Of course, in this process, the above diagrammatic rules must be satisfied.

Let us now indicate as $N_{mn}(r_{12})$ the sum of (the terms associate to) all the 1-2 subdiagrams of the type specified by the subscripts $mn$. Moreover, let us assume that $X_{mn}(r_{12})$ represents the sum of all the composite 1-2 subdiagrams of the type $mn$. The function $N_{mn}(r_{12})$ may be constructed by means of chain connection of the various elements $X_{mn}(r)$ with $X_{mn}(r)+N_{mn}(r)$. Due to the diagrammatic rules, only the following connections are possible:

$$X_{dd} + N_{mn}(r) \text{ with } X_{dd},\ X_{ee} \text{ or } X_{de},$$
$$X_{de} + N_{mn}(r) \text{ with } X_{dd} \text{ or } X_{de},$$
$$X_{ee} + N_{mn}(r) \text{ with } X_{dd} \text{ or } X_{de},$$
$$X_{cc} + N_{mn}(r) - \rho(r)/2 \text{ with } X_{cc} \text{ or } (-1/\nu)l.$$

The FHNC equations given by Eq. (2.19) are based on these combinations. The composite quantities $X_{mn}(r)$ are calculated in real space by the equations (2.21-24).

# APPENDIX B

In this appendix, we list in Table I–IV all combinations contributing to the four body elementary diagrams. As shown in Fig. (A.1), the $g$ bonds are combined as the diagrammatic rules and

$$g_{dde} = g_{dd} + g_{de} - 1 \qquad (B.1)$$

$$g_{epd} = g_{de} + g_{ee} \qquad (B.2)$$

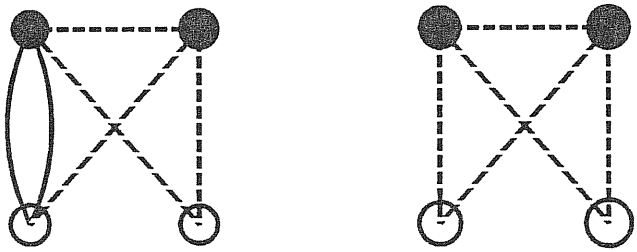

Figure 8.1: Four-body elementary diagrams

Table I: Combinations contributing to $E_{dd}$

| $c_i$ | A(13) | B(14) | C(23) | D(24) | E(34) |
|---|---|---|---|---|---|
| 1/2 | $g_{dd}-1$ | $g_{dd}-1$ | $g_{dd}-1$ | $g_{dd}-1$ | $g-1$ |
| 2 | $g_{de}$ | $g_{dd}-1$ | $g_{dd}-1$ | $g_{dd}-1$ | $g_{dde}$ |
| 1 | $g_{de}$ | $g_{de}$ | $g_{dd}-1$ | $g_{dd}-1$ | $g_{dd}-1$ |
| 1 | $g_{de}$ | $g_{dd}-1$ | $g_{dd}-1$ | $g_{de}$ | $g_{dd}-1$ |

Table II: The same as in Table I, for $E_{de}$

| $c_i$ | A(13) | B(14) | C(23) | D(24) | E(34) |
|---|---|---|---|---|---|
| 1 | $g_{de}$ | $g_{dd}-1$ | $g_{dd}-1$ | $g_{dd}-1$ | $g-1$ |
| 1 | $g_{ee}$ | $g_{dd}-1$ | $g_{dd}-1$ | $g_{dd}-1$ | $g_{dde}$ |
| 1 | $g_{de}$ | $g_{de}$ | $g_{dd}-1$ | $g_{dd}-1$ | $g_{dde}$ |
| 1 | $g_{de}$ | $g_{dd}-1$ | $g_{de}$ | $g_{dd}-1$ | $g_{dde}$ |
| 1 | $g_{de}$ | $g_{dd}-1$ | $g_{dd}-1$ | $g_{de}$ | $g_{dde}$ |
| 1 | $g_{ee}$ | $g_{de}$ | $g_{dd}-1$ | $g_{dd}-1$ | $g_{dd}-1$ |
| 1 | $g_{ee}$ | $g_{dd}-1$ | $g_{dd}-1$ | $g_{de}$ | $g_{dd}-1$ |
| 1 | $g_{de}$ | $g_{de}$ | $g_{de}$ | $g_{dd}-1$ | $g_{dd}-1$ |
| 1 | $g_{de}$ | $g_{dd}-1$ | $g_{de}$ | $g_{de}$ | $g_{dd}-1$ |
| -2 | $g_{cc}$ | $g_{cc}$ | $g_{dd}-1$ | $g_{dd}-1$ | $g_{cc}$ |

Table III: The same as in Table I, for $E_{ee}$

| $c_i$ | A(13) | B(14) | C(23) | D(24) | E(34) |
|---|---|---|---|---|---|
| 1 | $g_{de}$ | $g_{dd}-1$ | $g_{de}$ | $g_{dd}-1$ | $g-1$ |
| 1 | $g_{de}$ | $g_{dd}-1$ | $g_{dd}-1$ | $g_{de}$ | $g-1$ |
| 2 | $g_{de}$ | $g_{de}$ | $g_{de}$ | $g_{dd}-1$ | $g_{dde}$ |
| 2 | $g_{de}$ | $g_{de}$ | $g_{dd}-1$ | $g_{de}$ | $g_{dde}$ |
| 2 | $g_{ee}$ | $g_{dd}-1$ | $g_{de}$ | $g_{dd}-1$ | $g_{dde}$ |
| 2 | $g_{ee}$ | $g_{dd}-1$ | $g_{dd}-1$ | $g_{de}$ | $g_{dde}$ |
| 2 | $g_{ee}$ | $g_{de}$ | $g_{de}$ | $g_{dd}-1$ | $g_{dd}-1$ |
| 2 | $g_{ee}$ | $g_{de}$ | $g_{dd}-1$ | $g_{de}$ | $g_{dd}-1$ |
| 2 | $g_{ee}$ | $g_{dd}-1$ | $g_{de}$ | $g_{de}$ | $g_{dd}-1$ |
| 1 | $g_{ee}$ | $g_{dd}-1$ | $g_{dd}-1$ | $g_{ee}$ | $g_{dd}-1$ |
| 1 | $g_{de}$ | $g_{de}$ | $g_{de}$ | $g_{de}$ | $g_{dd}-1$ |
| -4 | $g_{cc}$ | $g_{cc}$ | $g_{de}$ | $g_{dd}-1$ | $g_{cc}$ |
| -2 | $g_{cc}$ | $g_{cc}$ | $g_{cc}$ | $g_{cc}$ | $g_{dd}-1$ |

Table IV: The same as in Table I, for $E_{cc}$

| $c_i$ | A(13) | B(14) | C(23) | D(24) | E(34) |
|---|---|---|---|---|---|
| 1 | $g_{cc}$ | $g_{dd}-1$ | $g_{dd}-1$ | $g_{cc}$ | $g_{cc}$ |
| 1 | $g_{cc}$ | $g_{dd}-1$ | $g_{cc}$ | $g_{dd}-1$ | $g_{dde}$ |
| 2 | $g_{cc}$ | $g_{de}$ | $g_{cc}$ | $g_{dd}-1$ | $g_{dd}-1$ |

Table V: As in Table I, but for $E_{\xi d}$

| $c_i$ | A(13) | B(14) | C(23) | D(24) | E(34) |
|---|---|---|---|---|---|
| 1/2 | $g_{\xi d}-1$ | $g_{\xi d}-1$ | $g_{dd}-1$ | $g_{dd}-1$ | $g-1$ |
| 1 | $g_{\xi e}$ | $g_{\xi d}-1$ | $g_{dd}-1$ | $g_{dd}-1$ | $g_{dde}$ |
| 1 | $g_{\xi d}-1$ | $g_{\xi d}-1$ | $g_{de}$ | $g_{dd}-1$ | $g_{dde}$ |
| 1/2 | $g_{\xi e}$ | $g_{\xi e}$ | $g_{dd}-1$ | $g_{dd}-1$ | $g_{dd}-1$ |
| 1/2 | $g_{\xi d}-1$ | $g_{\xi d}-1$ | $g_{de}$ | $g_{de}$ | $g_{dd}-1$ |
| 1 | $g_{\xi e}$ | $g_{\xi d}-1$ | $g_{dd}-1$ | $g_{de}$ | $g_{dd}-1$ |

Table VI: As in Table I, but for $E_{\xi cc}$

| $c_i$ | A(13) | B(14) | C(23) | D(24) | E(34) |
|---|---|---|---|---|---|
| 1 | $g_{\xi cc}$ | $g_{\xi d}-1$ | $g_{dd}-1$ | $g_{cc}$ | $g_{cc}$ |
| 1 | $g_{\xi cc}$ | $g_{\xi d}-1$ | $g_{cc}$ | $g_{dd}-1$ | $g_{dde}$ |
| 1 | $g_{\xi cc}$ | $g_{\xi e}$ | $g_{cc}$ | $g_{dd}-1$ | $g_{dd}-1$ |
| 1 | $g_{\xi cc}$ | $g_{\xi d}-1$ | $g_{cc}$ | $g_{de}$ | $g_{dd}-1$ |

A completely similar combinations are obtained for $E_{\xi e}$ by changing the first label $d$ of $G$ of $A(13)$ and $B(14)$ in Table IV into $\xi$. And combinations for $E_d$ are obtained by changing the first label $\xi$ of $G$ of $A(13)$ and $B(14)$ in Table X into $d$.

Table VII: As in Table I, but for $E_{\xi\xi}$

| $c_i$ | A(13) | B(14) | C(23) | D(24) | E(34) |
|---|---|---|---|---|---|
| 1/2 | $g_{\xi d}-1$ | $g_{\xi d}-1$ | $g_{\xi d}-1$ | $g_{\xi d}-1$ | $g-1$ |
| 2 | $g_{\xi e}$ | $g_{\xi d}-1$ | $g_{\xi d}-1$ | $g_{\xi d}-1$ | $g_{dde}$ |
| 1 | $g_{\xi e}$ | $g_{\xi e}$ | $g_{\xi d}-1$ | $g_{\xi d}-1$ | $g_{dd}-1$ |
| 1 | $g_{\xi e}$ | $g_{\xi d}-1$ | $g_{\xi d}-1$ | $g_{\xi e}$ | $g_{dd}-1$ |

Table VIII: As in Table I, but for $E_{\xi c\xi c}$

| $c_i$ | A(13) | B(14) | C(23) | D(24) | E(34) |
|---|---|---|---|---|---|
| 1 | $g_{\xi cc}$ | $g_{\xi d}-1$ | $g_{\xi d}-1$ | $g_{\xi cc}$ | $g_{cc}$ |
| 1 | $g_{\xi cc}$ | $g_{\xi d}-1$ | $g_{\xi cc}$ | $g_{\xi d}-1$ | $g_{dde}$ |
| 2 | $g_{\xi cc}$ | $g_{\xi e}$ | $g_{\xi cc}$ | $g_{\xi d}-1$ | $g_{dd}-1$ |

Table IX: Combinations contributing to $E_\xi$

| $c_i$ | A(13) | B(14) | C(23) | D(24) | E(34) | F(12) |
|---|---|---|---|---|---|---|
| 1/6 | $g_{\xi d}-1$ | $g_{\xi d}-1$ | $g_{\xi d}-1$ | $g_{dd}-1$ | $g_{dd}-1$ | $g-1$ |
| 1/6 | $g_{\xi d}-1$ | $g_{\xi d}-1$ | $g_{\xi d}-1$ | $g_{epd}$ | $g_{dd}-1$ | $g_{dde}$ |
| 1/6 | $g_{\xi d}-1$ | $g_{\xi d}-1$ | $g_{\xi d}-1$ | $g_{dd}-1$ | $g_{epd}$ | $g_{dde}$ |
| 1/6 | $g_{\xi d}-1$ | $g_{\xi d}-1$ | $g_{\xi d}-1$ | $g_{epd}$ | $g_{de}$ | $g_{dd}-1$ |
| 1/6 | $g_{\xi d}-1$ | $g_{\xi d}-1$ | $g_{\xi d}-1$ | $g_{de}$ | $g_{de}$ | $g_{de}$ |
| 1/2 | $g_{\xi d}-1$ | $g_{\xi d}-1$ | $g_{\xi d}-1$ | $g_{de}$ | $g_{ee}$ | $g_{dd}-1$ |
| -2/3 | $g_{\xi d}-1$ | $g_{\xi d}-1$ | $g_{\xi d}-1$ | $g_{cc}$ | $g_{cc}$ | $g_{cc}$ |
| 1/2 | $g_{\xi e}$ | $g_{\xi d}-1$ | $g_{\xi d}-1$ | $g_{dd}-1$ | $g_{dd}-1$ | $g-1$ |
| 1/2 | $g_{\xi e}$ | $g_{\xi d}-1$ | $g_{\xi d}-1$ | $g_{de}$ | $g_{dd}-1$ | $g_{dde}$ |
| 1/2 | $g_{\xi e}$ | $g_{\xi d}-1$ | $g_{\xi d}-1$ | $g_{dd}-1$ | $g_{de}$ | $g_{dde}$ |
| 1/2 | $g_{\xi e}$ | $g_{\xi d}-1$ | $g_{\xi d}-1$ | $g_{de}$ | $g_{de}$ | $g_{dd}-1$ |
| 1 | $g_{\xi e}$ | $g_{\xi e}$ | $g_{\xi d}-1$ | $g_{dd}-1$ | $g_{dd}-1$ | $g_{dde}$ |
| 1 | $g_{\xi e}$ | $g_{\xi e}$ | $g_{\xi d}-1$ | $g_{dd}-1$ | $g_{de}$ | $g_{dd}-1$ |

# Bibliography


[1] J. Hubbard, *Proc. Roy. Soc.* **A276**, 238 (1964), J. Hubbard, *Proc. Roy. Soc.* **A285**, 542 (1965).

[2] D. Vollhardt, *Rev. Mod. Phys.* **99**, 1196 (1984).

[3] E. H. Lieb and F. Y. Wu, *Phys. Rev. Lett.* **20**, 1445 (1968).

[4] P. W. Anderson, *Science* **235**, 1196 (1987).

[5] P. Fazekas, P.W. Anderson, *Phil. Mag.* **30**, 474 (1974).

[6] C. Gros, R.Joynt, T.M. Rice, *Phys. Rev.* **B36**, 381 (1987).

[7] J.E. Hirsh, *Phys. Rev.* **B31**, 4403 (1985); J.E. Hirsh and H.Q. Lin, *Phys. Rev. Lett.* **31**, 4403 (1989);

[8] S. Sorella, E. Tosatti, S. Baroni, R.Car and M. Parrinello, *Intern. J. Mod. Phys.* **B1**, 993 (1988); S. Sorella, S. Baroni, R.Car and M. Parrinello, *Europhys. Lett.* **8**, 663 (1989);

[9] H. Yokoyama, H.Shiba, *J. Phys. Soc. Jap.* **56**, 3570 (1987); H. Yokoyama, H.Shiba, *J. Phys. Soc. Jap.* **56**, 1490 (1987); H. Yokoyama, H.Shiba, *J. Phys. Soc. Jap.* **56**, 3582 (1987).

[10] E. Feenberg, *Theory of Quantum Fluids* (Academic, New York, 1969).

[11] J.W. Clark, in *Progress in Particle and Nuclear Physics*, ed. D.H. Wilkinson (Pergamon, Oxford, 1979), Vol.2.

[12] M. Viviani, S. Fantoni, S. Rosati, *Phys. Rev.* **C77**, 265, (1988).

[13] S. Fantoni and V. R. Pandharipande, *Phys. Rev.* **C37**, 1697 (1988); *Nucl. Phys.* **A427** 473 (1984); **A473** 234 (1987).

[14] S. Fantoni and S. Rosati, *Nuovo Cim.* **A25**, 593 (1975);

[15] E. Krotscheck and M.L. Ristig, *Nucl. Phys.* **A242**, 389 (1975).

[16] W. Metzner, D. Vollhardt, *Phys. Rev. Lett.* **59**, 121 (1987); F. Gebhardt, D. Vollhardt, *Phys. Rev. Lett.* **59**, 1472 (1987).

[17] J.C. Owen and G. Ripka, *Phys. Rev.* **B25**, 4914 (1982).

[18] C.H. Yang, J.W. Clark,*Nucl. Phys.* **A174**, 49 (1971); T. C. Paulick and C.E. Campbell, *Phys. Rev.* **B16**, 2000 (1977); E. Krotscheck, J.W. Clark, *Nucl. Phys.* **A333**, 77 (1980).

[19] R. B. Winringa, V. Fiks, A. Fabrocini, *Phys. Rev.* **C38**, 1010 (1988).

[20] T.A. Kaplan, P. Horsh and P. Fulde, *Phys. Rev. Lett.* **49**, 889 (1982).

[21] D. Baeriswy, in *Nonlinearity of Condensed Matter Physics*, eds. A.R.Bishop et al, (Springer, Berlin) p183 (1987).

[22] S. Rosati, From nuclei to particles, (1981) p73.

[23] S. Fantoni, X.Q. Wang, E. Tosatti and Yu Lu, *Physica C* **153-155**, 1255(1988).

[24] V.R.Pandharipande and R.B. Wiringa, *Rev. Mod. Phys.* **51**, 821 (1979).

[25] P. Fazekas and K. Penc, *Intern. J. Mod. Phys.* **B1**, 1021 (1988).

[26] S. Fantoni and S. Rosati, *Nuovo Cim.* **A20**, 179 (1974).

[27] S. Fantoni, *Nuovo Cim.* **A44**, 191 (1978).

[28] B. Friedman and V.R. Pandaripande, *Phys. Lett.* **100B**, 205 (1981).

[29] E. Tosatti, (unpublished).

[30] A. Parola, S. Sorrela, E.Tosatti, M. Parrinello (to be published).

[31] J.R. Schrieffer, X.G. Wen, and S.C. Zhang, *Phys. Rev.* **B39**, 11663 (1989).

[32] X.Q. Wang, S. Fantoni, E. Tosatti, Yu Lu, (in preparation).

[33] Q.N. Usmani, B. Friedman and V.R. Pandharipande, *Phys. Rev.* **B25**, 4502 (1982).

[34] M. Viviani, A. Buendia, A. Fabrocini and S. Rosati, *Nuovo Cim.* **D8**, 561 (1986).

[35] T.C. Paulick and C.E. Campbell, *Physics Rev.* **B16**, 2000 (1977).

[36] J. Solyom, *Advances in Physics* **28**, 201 (1979).

[37] F.C. Zhang, C. Gros, T.M. Rice and H. Shiba, *Supercond. Sci. Technol.* **1**, 36 (1988).

[38] V.J. Emery, *Phys. Rev. Lett.* **60**, 379 (1988).

[39] S.Fantoni, *Nucl. Phys.* **54**, 2684 (1981).

[40] X.Q. Wang, S. Fantoni, E. Tosatti, Yu Lu, and M. Viviani, (to be submitted to Phys. Rev. B).